

1 **Quantifying the response of water and carbon balances to land**  
2 **cover and climate extremes across Germany.**

3 Karim Pyarali<sup>1,2\*</sup>, Lulu Zhang<sup>2\*</sup>, Ning Liu<sup>4</sup>, Abdulhakeem Al-Qubati<sup>1,2</sup> and Ge Sun<sup>3\*</sup>

4 <sup>1</sup>Technische Universität Dresden, Helmholtzstr. 10, 01069, Dresden, Germany.

5 <sup>2</sup>United Nations University, Institute for Integrated Management of Material Fluxes and of Resources, Ammonstrasse  
6 74, 01067, Dresden, Germany.

7 <sup>3</sup>Eastern Forest Environmental Threat Assessment Center, Southern Research Station, USDA Forest Service, Research  
8 Triangle Park, NC 27713, USA.

9 <sup>4</sup>CSIRO Environment, Canberra ACT 2601.

10 \*Corresponding authors: Karim Pyarali ([karim.pyarali@tu-dresden.de](mailto:karim.pyarali@tu-dresden.de)); Lulu Zhang ([lzhang@unu.edu](mailto:lzhang@unu.edu)); Ge Sun  
11 ([Ge.Sun@usda.gov](mailto:Ge.Sun@usda.gov))

12

13 **Abstract.** Land cover and extreme weather events are closely connected to ecosystem services like water yield and  
14 carbon sequestration. Understanding how carbon and water respond to human disturbances is critical for managing  
15 these resources and realize desired ecosystem services at the national level. The monthly scale ecosystem model,  
16 Water Supply Stress Index (WaSSI), was tested and applied across Germany for mapping carbon and water balances  
17 from 2001 to 2019. We estimated that ecosystems in Germany generate 84.86 billion m<sup>3</sup> of water yield and sequester  
18 106.03 Tg of carbon annually on average. Most of the precipitation was lost as evapotranspiration in eastern states  
19 that were comparatively drier in river flows than the rest of the country. Croplands, urban areas and Evergreen Needle  
20 Forests (ENF) provide 82.5% of the national water yield, while the forest lands share the majority (56.3%) of land  
21 carbon sequestration altogether. Our simulation results highlight the importance of sparse land covers (e.g. wetlands)  
22 in carbon sequestration. Findings also suggest that national water yield and carbon balances are sensitive to extreme  
23 events such as the floods in 2002 and 2013 and the extreme drought in 2003 and 2018. We found that hydrologic  
24 buffers from the previous year played an important role in mitigating negative impacts on both carbon and water  
25 availability. This study highlights that, when integrated with local data, a relatively simple modelling approach is  
26 adequate to quantify the coupled water and carbon responses to climatic and land cover variability at a large scale.  
27 We conclude that land management of both forests and croplands is vital to sustain ecosystem services under a  
28 changing climate at regional to national levels.

## 29 1. Introduction

30 Ecosystem services such as water yield and carbon sequestration are intimately linked with land cover and climate  
31 extremes. The two key ecosystem services support life and economic activity (Morales et al., 2005). The tightly  
32 coupled links between water and carbon cycles through parameters such as precipitation, temperature,  
33 evapotranspiration (ET), and ecosystem services are well recognized (Beer et al., 2007; Sun et al., 2011). However, it  
34 is still unclear how changes in land cover and climate extremes have impacted these services in Germany at a national  
35 level. These services are challenging to measure directly, but an ecosystem services model can be applied to estimate  
36 them across the German landscape at a sub-basin scale.

37 Changes in land cover are driven by multiple interconnected reasons, two of them are improving living standards and  
38 population growth (Allan et al., 2022). Studies have shown that land cover change greatly reduces ecosystem services,  
39 but the impact varies spatially and temporally (Hasan et al., 2020). According to Pandey & Ghosh (2023), and Salerno  
40 et al. (2018), urbanization disrupts regulating service for e.g., water purification, soil retention, and climate regulation.  
41 On the other hand, Arowolo et al. (2018) and Cui et al. (2021) observed that expansion of cropland often increases  
42 goods from provisioning services such as food, fodder and water yield. A recent survey in 2022 from the German  
43 national forest inventory found that since 2017, the German forest has become a source of carbon dioxide, instead of  
44 being a sink. The reason behind the change in ecosystem functions is the high loss of living biomass due to climate  
45 change and low forest growth (Fourth Federal Forest Inventory 2022, 2024).

46 Another environmental phenomena that impact ecosystem services are extreme climate events (e.g. droughts &  
47 extreme precipitation). Catastrophic weather events not only made countries in the Global South but also in Global  
48 North vulnerable. Germany's 2021 summer flood resulted in a loss of 220 lives and US\$ 40 Billion (Schumacher,  
49 2022); the incurred damages from the 2003 drought, primarily on agriculture, were approximately US\$13 Billion  
50 across Europe (Eisenreich, 2005). Germany has seen an increase in the intensity and frequency of heavy rainfall, more  
51 in winter than in summer. The air temperatures are also projected to rise by 1.6 to 3.8°C by 2080 (Schröter et al.,  
52 2005). A shift in precipitation season has been observed, which will potentially increase the risks of floods during  
53 winter and decrease the water supply during summer periods (Schröter et al., 2005). The extreme events are changing  
54 due to climate change. Their impacts may reduce terrestrial carbon uptake or gross primary productivity (GPP)  
55 (Williams et al., 2014), which negatively affects other factors within the co-evolved processes of carbon-water cycle  
56 in an integrated terrestrial system (Zhang et al., 2018). Potentially leading to adverse effects on regional food and  
57 livelihood security.

58 Although ecosystem services are essential and well-recognized in Germany, national-scale studies on both carbon and  
59 water yield are still lacking. There are multiple studies that focus on a specific land cover type or specific ecosystem  
60 services at the European, national or subnational scales. For example, Potter & Pass (2024) estimated the changes in

61 net primary productivity (NEP or carbon sequestration) for Western Europe, including Germany. Gutsch et al. (2018)  
62 assessed German forest ecosystem services under climate change and different management scenarios. Their results  
63 showed that climate change has negative impacts on water percolation and positive impacts on carbon sequestration.  
64 Using agricultural long-term field experiments, carbon sequestration was projected to increase in the southern parts  
65 of Germany, indicating higher productivity, and decrease in central and east Germany where poor soil will further  
66 reduce the productivity (Donmez et al., 2024). Other studies used regional analysis to assess water or carbon cycles  
67 (Al-Qubati et al., 2023; Prescher et al., 2010; Ungaro et al., 2021; Wu et al., 2021). The lack of integrated water-  
68 carbon cycles assessment hampers deriving national or regional adaptive land management strategies to alleviate the  
69 adverse impacts resulting from environmental and climate change, particularly in the long term.

70 Furthermore, we observed a varied response of the coupled water-carbon cycle to changes in land cover and climate  
71 (Cheng et al., 2017; Jung et al., 2017; Zeng et al., 2018). The variation is manifested by the coupled mechanisms  
72 occurring at multiple timescales. These may be short-term leaf-gas exchanges, monthly or annual ET and carbon  
73 accumulation, and long-term water yield and species composition. This emphasises that a single type of observation  
74 is not sufficient to provide the robust validation needed to address the response of water and carbon cycles to  
75 environmental disturbances or climate shocks (Margulis et al., 2006). Gentine et al. (2019) argued that terrestrial  
76 water-carbon cycles must be investigated as an integrated system. They recognized the importance of incorporating  
77 multiple observations on different timescales from various sources to better validate model simulations, which may  
78 reduce uncertainties, mitigate bias, and provide better predictions. Unfortunately, the suggested approach is seldomly  
79 applied in hydrological modelling (e.g. G. Sun et al., 2011, 2023; J. Zhang et al., 2022; Y. Zhang et al., 2016). Thus,  
80 impeding the improvement of our predictive ability to quantify the potential water-carbon changes and consequences  
81 that are vital to effective policy decision-making for developing climate adaptation and mitigation strategies.  
82 Therefore, we integrated multi-timescale observations and information sources in our model to validate simulated  
83 water yield and carbon sequestration. We used gauged river discharge (Q), in-situ measured ET and GPP from eddy  
84 flux towers, and remotely sensed ET and GPP data for model validation.

85 In this study, WaSSI, an ecosystem service model, was applied on a monthly and subbasin (804) resolution to simulate  
86 the water and carbon processes across the different land covers within Germany (Sun et al., 2011). The model has  
87 been used globally for various purposes and under different climatic and socioeconomic conditions (Averyt et al.,  
88 2011; Caldwell et al., 2011, 2014, 2012; N. Liu et al., 2020; G. Sun et al., 2011; S. Sun et al., 2015; McNulty et al.,  
89 2016;) in countries like the United States of America, Rwanda, Australia, Turkiye, Nepal and China (Chen et al., 2024;  
90 Jin et al., 2025; Liu, 2017; Liu et al., 2013; McNulty et al., 2016; Sun et al., 2011). By validating the WaSSI model,  
91 we aim to have an improved understanding of the response of water-carbon cycles on German land cover with climate  
92 variability at a watershed scale. Furthermore, we focus on three questions: (i) How did ET, water yield and NEP vary  
93 over time and space? (ii) How did different land cover contribute to water yield and carbon sequestration? and (iii) to  
94 what extent and how sensitive are the two ecosystem services to extreme weather events?

## 95 **2. Methodology and Data**

96 The WaSSI model merges the water and carbon cycle using water use efficiency (WUE) parameters estimated from  
97 global eddy flux observations. It is made up of two components: a hydrological and a carbon sub-model. The required  
98 inputs are precipitation, temperature, digital elevation model, land cover, fractional impervious cover, leaf area index  
99 (LAI), and soil parameters, while the outputs are Q, ET, GPP, and net ecosystem exchange (NEE) (Liu, 2017).  
100 Transboundary inflows and outflows were not accounted in this study; therefore, watersheds close to Germany's  
101 boundary, which accumulated their flow across the border, were not considered.

102 The WaSSI model estimates land cover-specific water yield (mm per month), which can be aggregated as flow volume  
103 downstream (m<sup>3</sup> per month) for any individual watersheds. The hydrologic fluxes estimated are snow melt, snow  
104 accumulation, soil storage, surface flow, base flow, routed flow accumulation, and ET (Sun et al., 2011). The model  
105 employs a conceptual method (McCabe & Wolock, 1999) that uses the monthly average temperature and mean average  
106 elevation of a watershed to partition precipitation into rainfall and snowfall, estimate the rate of snow melt, and  
107 calculate the mean monthly snow water equivalent for each watershed (Caldwell et al., 2012). The Sacramento Soil  
108 Moisture Accounting (SAC-SMA) model was used for soil and runoff parameters, which runs infiltration, baseflow,

109 surface runoff, and soil moisture processes, while also constraints ET estimates based on soil water content. For ET  
 110 estimations, we used the Type II regression model from (Fang et al., 2015), where the ET model was developed using  
 111 quality-controlled global data from more than 200 eddy flux sites (Pastorello et al., 2020), incorporating the three most  
 112 commonly available biophysical parameters precipitation (P), potential ET (PET) (Temperature based) and LAI in the  
 113 following equation:

$$ET = -4.79 + 0.75PET + 3.92LAI + 0.04P \quad (1)$$

114 WaSSI estimates three main components of the carbon cycles: (i) GPP or total carbon uptake, (ii) ecosystem  
 115 respiration ( $Re$ ) representing carbon loss, and (iii) Net Ecosystem Productivity (NEP) or negative Net Ecosystem  
 116 Exchange (NEE) or carbon sequestration:

$$NEP = -NEE = -(Re - GPP) \quad (2)$$

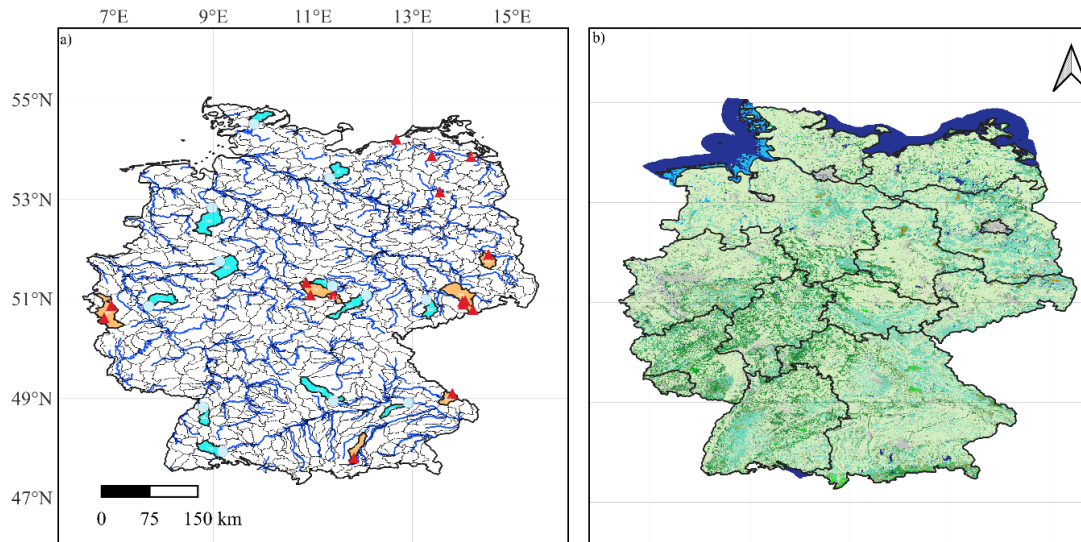
117 Furthermore, a closely coupled relationship between ET and GPP has been found in multiple studies (Law et al., 2002;  
 118 Sun et al., 2011), as presented in Equation 3. In the WaSSI model, according to G. Sun et al., (2011), the relationship  
 119 of monthly GPP with ET was estimated using linear regression for each land cover. Furthermore, land cover-specific  
 120 WUE parameters were used, which were estimated using 142 eddy flux tower data (Zhang et al., 2016). Similarly, the  
 121  $Re$  from heterotrophic and autotrophic bacteria can be estimated using Equation 4, where regression coefficients are  
 122 estimated from eddy flux data. The coefficient (a, m, and n) values used in this study are provided in Table S1.

$$GPP = a \times ET \quad (3)$$

$$Re = m + n \times GPP \quad (4)$$

## 123 2.1. Model Validation

124 We validated the model outputs using both in-situ observed data (e.g., stream discharge data from gauge stations and  
 125 ET eddy flux data) and remotely sensed data (e.g., ET and GPP estimates from satellites). The temporal resolution of  
 126 the WaSSI model output was monthly. The discharge was validated across the entire available temporal period, during  
 127 dry-hot years and during wet-cold years. Twelve upstream watersheds were nominated for validation spread across  
 128 Germany (Fig. 1). The chosen upstream stations were selected to ensure spatial coverage across Germany, representing  
 129 the country's major climatic zones, land use, and land cover types. Stations with long and continuous discharge records  
 130 were prioritised. The performance criteria to determine the accuracy of outputs are model bias (%), coefficient of  
 131 determination ( $R^2$ ), scatter plots, Nash-Sutcliffe efficiency (NSE), and Kling-Gupta efficiency (KGE). The estimated  
 132 ET was validated against data on different timescales. Simulated ET was compared with daily data from multiple eddy  
 133 flux towers, monthly ET from Moderate Resolution Imaging Spectroradiometer (MODIS) (MOD16A2GF) (Running  
 134 et al., 2019b), and watershed-specific water balance values, which were calculated by subtracting discharge from  
 135 precipitation, on a monthly and annual timescale. Depending on the validation datasets, values were summed to either  
 136 monthly or annual timesteps. For carbon, we compared the GPP estimates with GPP measurements from eddy flux  
 137 towers, MODIS GPP (MOD17A2HGF) and Copernicus Global Land Service (CGLS) GPP (Running et al., 2019a;  
 138 Smets et al., 2019). A monthly land cover-specific validation was conducted between modelled GPP and observed  
 139 GPP. Where observed GPP estimates were developed using the daytime partitioning method (GPP\_DT\_VUT\_REF).  
 140 Further details for each validation dataset are provided in the following section 2.3. Since the observed data from the  
 141 gauge stations and eddy flux towers did not overlap, therefore, joint evaluation at the same subbasin for both Q and  
 142 ET was not possible in this study.



### Legend

GRDC Gauges	State Boundaries	Evergreen Needleleaf Forests
Eddy Flux Towers	<b>Land Cover</b>	Mixed Forests
Q Validation Watersheds	<b>Classes</b>	Grasslands
ET Validation Watersheds	Urban	Closed Shrublands
Watersheds	Croplands	Open Shrublands
River Network	Deciduous Broadleaf Forests	Wetlands
		Water Bodies

143

144 **Figure 1:** A map of the study area presenting **a)** Germany's boundaries with all the 804 watersheds delineated, Global  
 145 Runoff Data Center's (GRDC) gauge station locations, major rivers, eddy flux tower sites and representative  
 146 watersheds for streamflow (Q) and evapotranspiration (ET) validation and **b)** Germany's land cover and state  
 147 boundaries.

## 148 2.2. Input Data

### 149 2.2.1. Study Area

150 Germany, with an area of 357,168 km<sup>2</sup>, consists of sixteen states. Approximately 83.5 million people reside across  
 151 five major river basins that fall within Germany (Rhine, Danube, Elbe, Weser, and Ems). Due to cross-boundary flows,  
 152 Germany has bilateral water treaties with all of its neighbours. The climatic conditions span from maritime to  
 153 continental. The annual mean temperature ranges from 9 to 11°C, and the annual precipitation ranges from 450 mm  
 154 to 970 mm (Kosanic et al., 2019). The land use is dominated by agriculture (61%) and forests (29%). Furthermore,  
 155 the built-up area (6%) is continuously expanding as cities grow due to urbanization. Socio-economically there is a  
 156 clear divide between the Eastern and Western states due to the Soviet-era policies. In this study, Germany was  
 157 delineated into 804 subbasins as the modeling units using a high-resolution digital elevation model (Fig. 1).

### 158 2.2.2. Climate Data

159 Climate data (i.e., precipitation and temperature) is sourced from Germany's national meteorological service (DWD,  
 160 2018). Datasets have a spatial resolution of 1km and a temporal resolution of months. The gridded data are prepared  
 161 by estimating monthly deviations for each station, which are then interpolated using inverse squared distance weighted  
 162 interpolation and transformed back into real values using reference grids (Kaspar et al., 2013).

### 163 2.2.3. Land cover classification

164 CORINE land cover (CLC) map of 2018 with a 100 m spatial resolution was used in this study (EEA, 2021). Validation  
165 studies showed that it can capture land cover with an accuracy of 85% (Büttner et al., 2021; Keil, 2017). This study  
166 reclassified land cover into 10 major classes. Table S2 shows the range of CLC classes that were merged along with  
167 their percentage across Germany. The selection of 10 classes was based on the availability of water-use efficiency  
168 (WUE) parameters. These 10 classes encompass all dominant ecosystem types across the study.

### 169 2.2.4. Leaf Area Index

170 Climate Data Record's (CDR) Vegetation (VGT) sensor LAI was used. The data is available from 2001 to 2014, with  
171 a 10-day temporal and 1km spatial resolution. All pixels with an invalid LAI status were removed during quality  
172 control. Invalid LAI status refers to pixel values that do not fall within an expected range (Verger et al., 2018).  
173 Validation studies of this product showed that it underestimates ground data with a bias of 0.31 and a correlation of  
174 0.72, while against multiple satellite datasets, it overestimates with biases ranging between 0.03 (for MODIS) to 0.36  
175 (for GLOBCARBON) (Camacho & Cernicharo, 2014).

### 176 2.2.5. Fractional impervious cover and soil data

177 The fractional impervious cover is derived from the Global Man-made Impervious Surface (GMIS) dataset (Brown  
178 de Colstoun et al., 2017). It has a spatial resolution of 30m.

179 Digital soil map BUEK 200 was used to estimate eleven soil parameters following Y. Zhang et al. (2011) and Anderson  
180 et al. (2006). Land cover and soil properties were used to obtain the curve number (CN) that controls the partitioning  
181 of soil into upper and lower zones. The water allocation between tensed and free water storage is determined by soil  
182 composition. The final product has a spatial resolution of 500 m.

## 183 2.3. Validation Data

### 184 2.3.1. Stream Discharge Data

185 The discharge data used for validation are sourced from the Global Runoff Data Center (GRDC). Twelve upstream  
186 stations were identified from a large group of stations for validation of discharge in this work. The selection focused  
187 on upstream watersheds that have less anthropogenic influence (e.g. dams), thus representing natural processes  
188 reasonably well. Furthermore, these stations had continuous long-term discharge data, they represent different climatic  
189 zones in Germany, and they capture diverse land use and land cover types. The location of stations can be observed  
190 in Fig. 1, while their names and ID are provided in Table S3.

### 191 2.3.2. Eddy Flux ET and GPP

192 ET and GPP in-situ measurements were acquired from the FLUXNET2015 database (Pastorello et al., 2020). The data  
193 available is quality-controlled. The gaps within the data are filled and corrected following standardised  
194 FLUXNET2015 procedures, which apply algorithms to ensure temporal continuity and consistent flux measurements.  
195 Furthermore, the energy balance closure correction factors (EBC\_CF) were used to correct these datasets. The  
196 EBC\_CF were estimated using three different methods each assuming that the Bowen ratio holds true. In this study,  
197 monthly latent heat turbulent flux (LE) was converted to ET with and without energy closure corrections and GPP  
198 was calculated using the daytime partitioning method (Pastorello et al., 2020).

### 199 2.3.3. MODIS ET and GPP Data

200 The MODIS ET product MOD16A2GF is employed in this work (Running et al., 2019b). The remote sensing data is  
201 used to compare the spatial variation of model output. MODIS has a spatial resolution of 500m and a temporal  
202 resolution of 8-day. The ET estimation follows the Penman-Monteith equation (Running et al., 2019b). The product  
203 has been comprehensively validated in multiple studies (Kim et al., 2012; Liu et al., 2015; Trambauer et al., 2014;  
204 Velpuri et al., 2013) and used to evaluate the output of hydrological models (Sun et al., 2011). This study used a  
205 monthly sum of ET values and spatial average calculated on a sub-watershed scale.

206 The gap-filled GPP product employed in this study is MOD17A2HGF, with a spatial resolution of 500m and a  
207 temporal resolution of 8-day (Running et al., 2019a). It follows Monteith's logic and uses land cover specific light  
208 use efficiency ( $\epsilon$ ), fraction of absorbed photosynthetically active radiation (FPAR), incident photosynthetically active  
209 radiation (IPAR), the deficit of vapor pressure, and minimum air temperature (Running et al., 2019a). Insights on the  
210 application and validation of MODIS-GPP are provided in multiple studies (Liu et al., 2015; Sun et al., 2011; Turner  
211 et al., 2006; Wang et al., 2017; Zhu et al., 2018).

212 CGLS GPP are derived from the Gross Dry Matter Productivity (GDMP) values (Smets et al., 2019). We used the  
213 version 2 product from SPOT/VGT and PROBA-V satellites to evaluate the model GPP estimates for the period of  
214 2001 – 2019. The GDMP product has a spatial and temporal resolution of 1-km and 10-day. It represents the additional  
215 gross dry biomass stored in vegetation, which could be converted into gross carbon uptake by multiplying it with a  
216 scaling factor of 0.45 gC/gDM (Smets et al., 2019):.

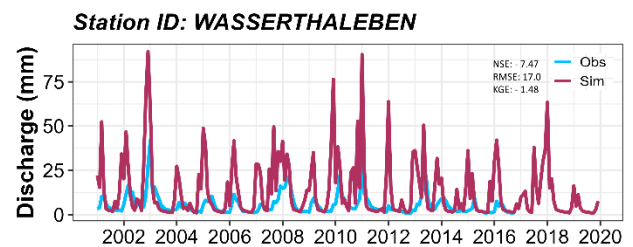
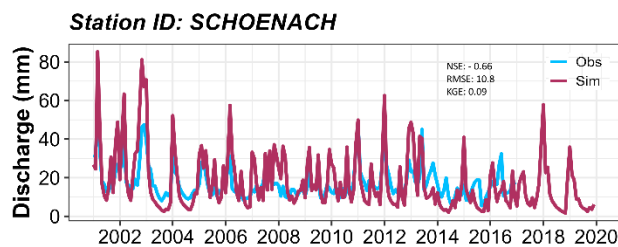
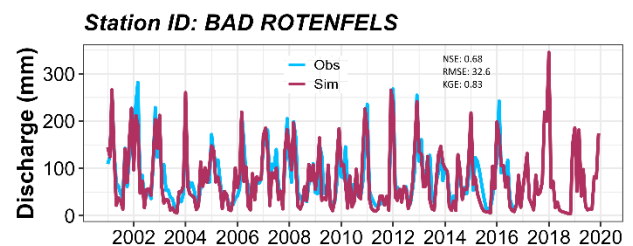
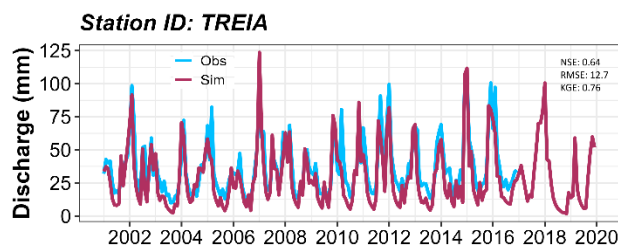
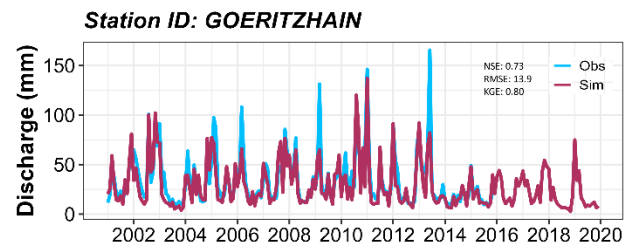
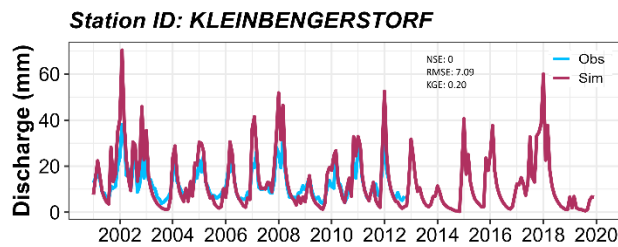
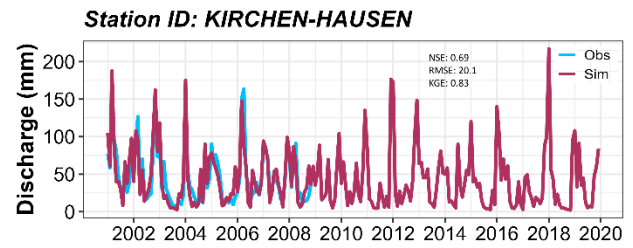
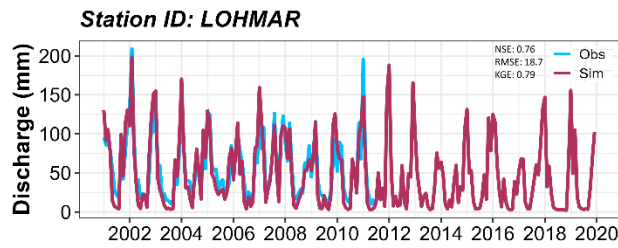
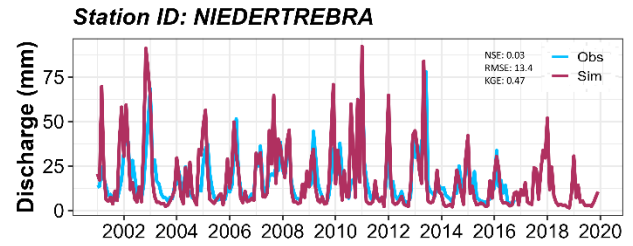
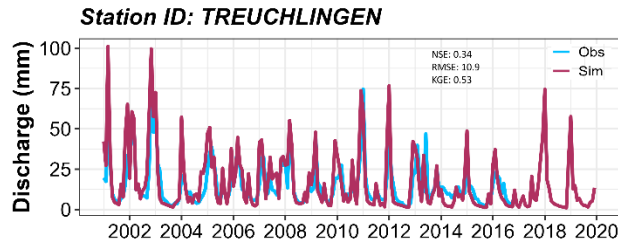
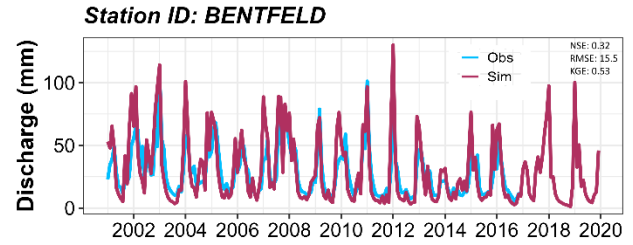
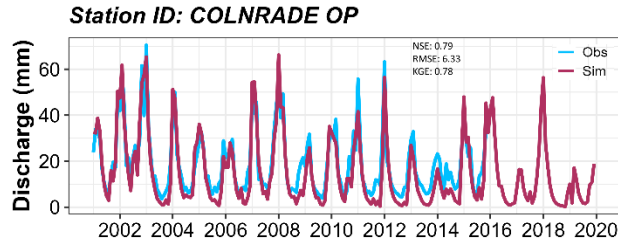
$$GPP (gC m^{-2} day^{-1}) = GDMP (kg DM ha^{-1} day^{-1}) * 0.45 * 0.1 \quad (5)$$

### 217 3. Results

#### 218 3.1. Model Validation

##### 219 3.1.1. Discharge Validation

220 The hydrograph plots, ordered by decreasing watershed area, reveal that the model, in general, is able to simulate the  
221 monthly flows reasonably well (Fig. 2). Furthermore, the model discharge validated on a monthly scale gives KGE  
222 for eight out of the twelve watersheds above 0.5 and NSE for six out of twelve watersheds greater than 0.6, as shown  
223 in Table S3. While on an annual scale the values of model bias (%) for eleven out of the twelve stations are between  
224 -25% to 25% and for  $R^2$  ten out of twelve stations are above 0.60, as presented in Table S4. The model also performs  
225 reasonably well during dry-hot and wet-cold years, as shown in Table S4. The scatter plot between modelled and  
226 observed discharge, across the twelve watersheds on both annual and monthly scales, is presented in Fig. S1. The plot  
227 shows high correlation between the two datasets suggesting the model performs reasonably well. Except for the  
228 Wasserthaleben station, where the model performance is weak with bias equal to 131.8 % and annual  $R^2$  of 0.18.

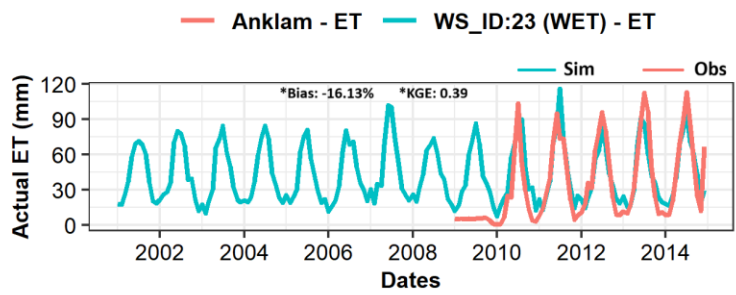
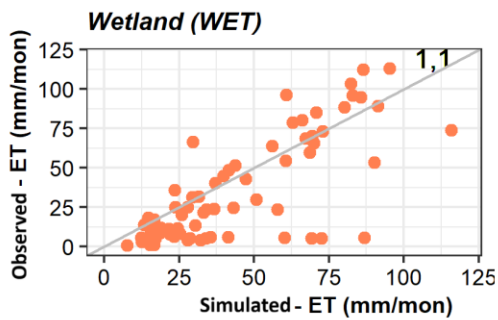
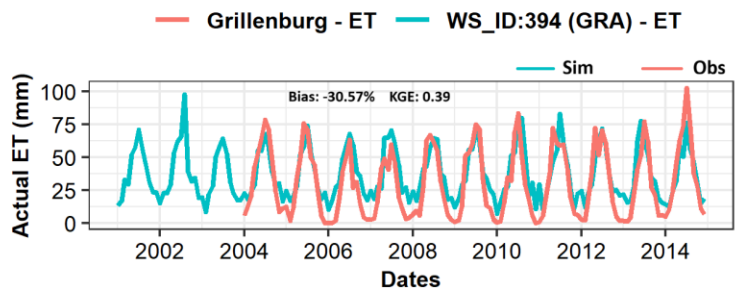
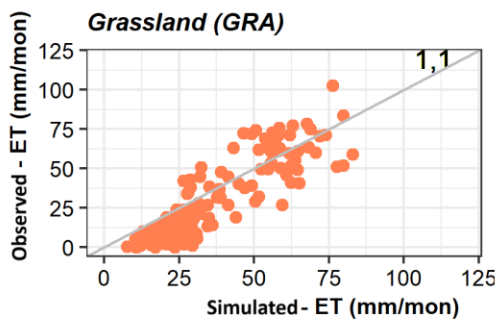
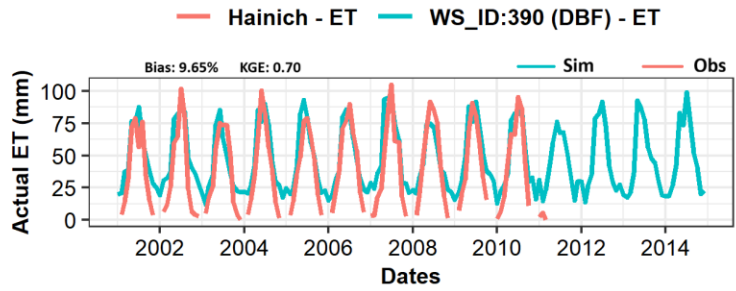
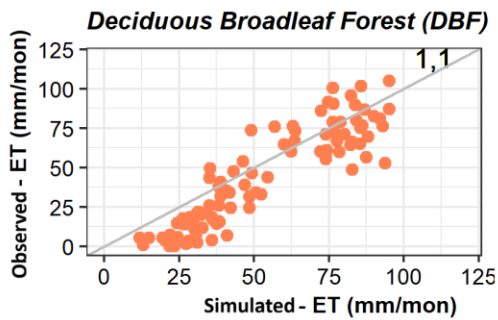
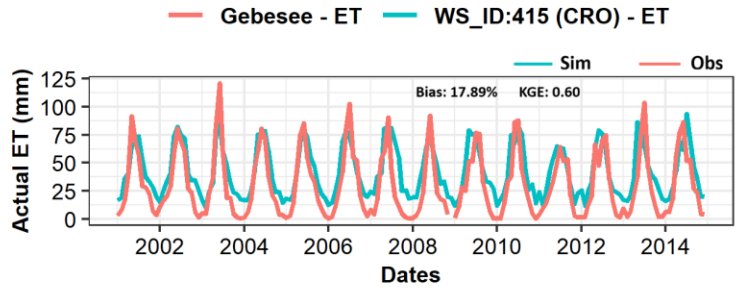
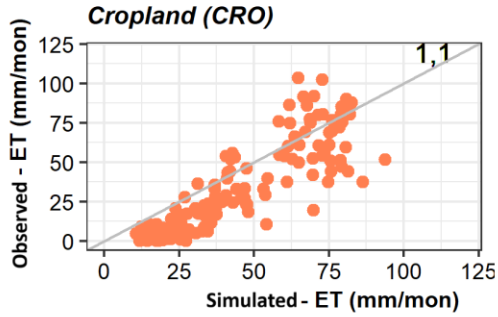
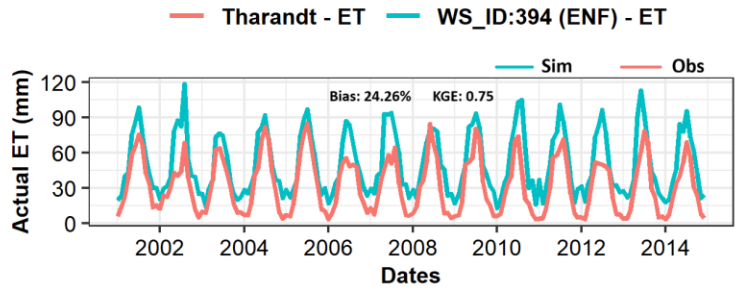
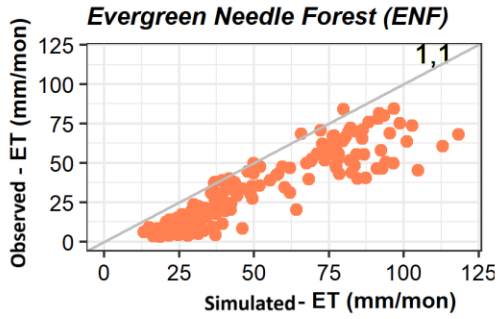


230 **Figure 2:** Monthly discharge time series from WaSSI simulation in mm (maroon) plotted against observed gauge  
231 station flow in mm (blue) during 2000-2020. The panels are arranged based on the corresponding watershed area,  
232 starting from the largest to the smallest.

### 233 3.1.2. ET Validation

234 Monthly land cover specific validation of simulated ET against EC ET is presented in Fig. 3. The ET estimates are  
235 captured reasonably well by the model as the points in the scatter plot generally stayed close to the 1:1 line except for  
236 Grassland. The detailed validation results are provided in Table S5. Ten out of eleven watersheds have an  $R^2$  value  $>$   
237 0.6 and a correlation  $>$  0.75. Seven out of eleven watersheds have a model bias (%) between -25% to 25%, and KGE  
238 estimate  $\geq$  0.6. Discrepancies are found in Lackenberg station with a bias of 52.4 %, and in general we observed that  
239 WaSSI model tends to slightly overestimate ET during winter. Overall, the model is able to capture ET values  
240 reasonably well across different land covers within Germany (Fig. S2a).

241 WaSSI ET on an interannual scale showed that it can satisfactorily simulate the variability of ET captured by MODIS  
242 across Germany, as shown in Fig S2b-c. The model mostly underestimated ET in southern and northwestern Germany,  
243 while slightly overestimating the ET in mid-western and eastern Germany. When the simulated ET is assessed against  
244 ET estimates as precipitation minus observed discharge ( $P-Q_{\text{observed}}$ ) interannually, the mean annual biases for all the  
245 twelve watersheds are within  $\pm 25\%$  threshold. Eight out of the twelve watersheds have biases within  $\pm 10\%$ , indicating  
246 a very good model performance (Table S6).



248 **Figure 3:** Land cover specific simulated ET validation (WS\_ID) against corrected eddy flux ET data. The line running  
 249 diagonally through the scatter plot is a 1:1 line. The performance metrics provided were calculated using corrected  
 250 ET for all stations except for Anklam (wetland).

251 **3.1.3. GPP Validation**

252 The results showed that nine out of fourteen watersheds have a model bias within  $\pm 25\%$ , twelve had  $R^2 > 0.6$ , seven  
 253 had  $NSE > 0.5$ , six have  $KGE > 0.5$ , and all the watersheds have a correlation  $> 0.6$ , as shown in Table 1. Furthermore,  
 254 the results show that simulated GPP from WaSSI are higher compared to the remotely sensed GPP estimates from  
 255 Copernicus and MODIS satellite by approximately 7% and 16%, respectively. The difference, correlation and  
 256 regression between simulated GPP and remotely sensed GPP is shown in Fig. S3.

257 **Table 1:** Monthly validation of WaSSI-GPP against EC-GPP. Stations are grouped for different land covers e.g.  
 258 cropland (CRO), deciduous broadleaf forest (DBF), ENF, grassland (GRA) and wetland (WET).

259

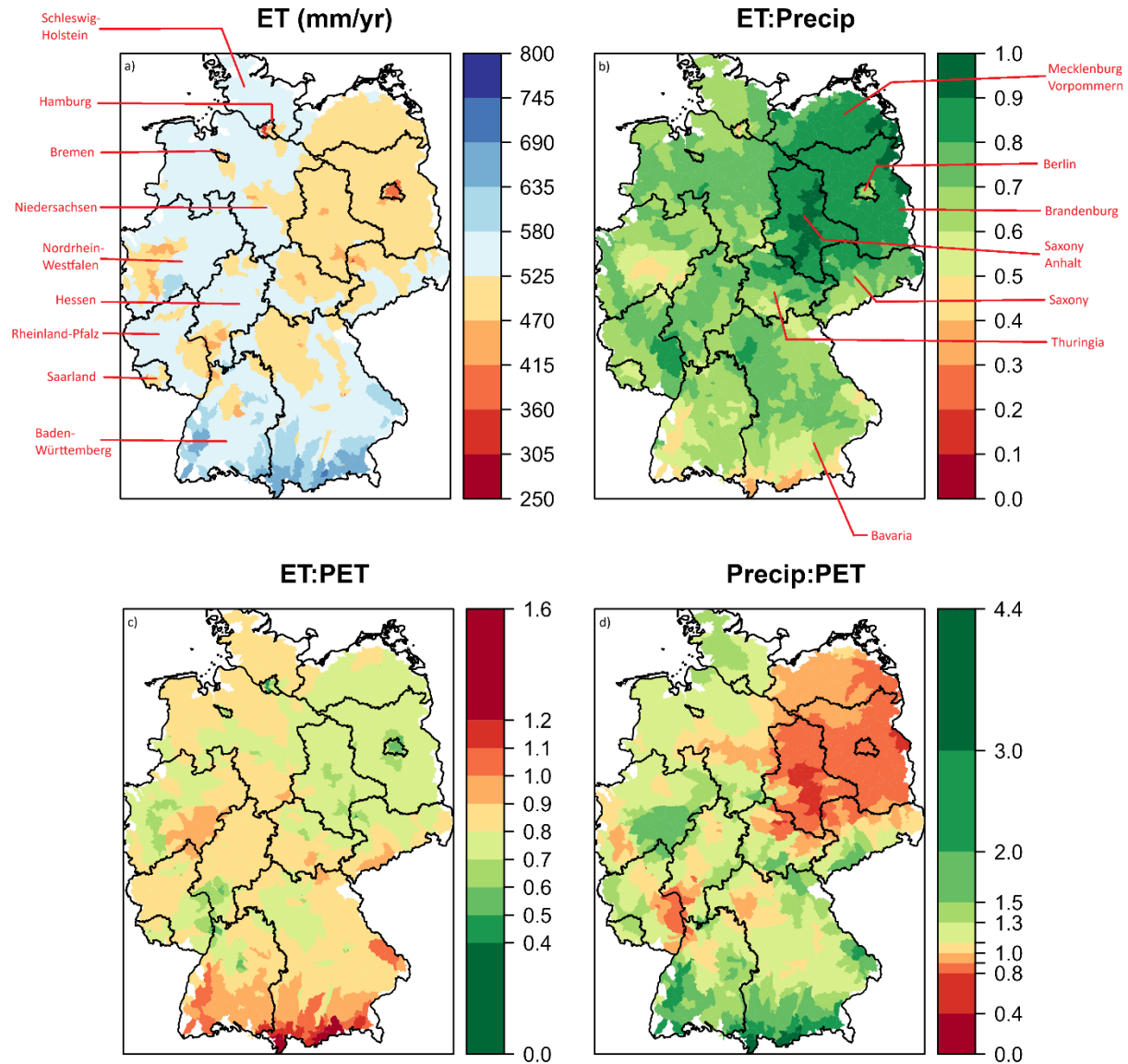
Eddy Flux Tower	Watershed ID	Land cover	Model bias %	R <sup>2</sup>	Corr	NSE	KGE
Selhausen Juelich	457	CRO	-15.94	0.65	0.81	0.45	0.33
Klingenberg	394		8.34	0.38	0.62	0.37	0.37
Gebsee	415		13.54	0.48	0.69	0.41	0.35
Hainich	390	DBF	8.28	0.84	0.92	0.73	0.57
Leinefelde	390		3.19	0.87	0.93	0.75	0.57
Lackenberg	631		224.09	0.83	0.91	-5.82	-1.51
Oberbärenburg	394	ENF	-13.4	0.86	0.93	0.74	0.59
Tharandt	394		-19.7	0.89	0.94	0.73	0.59
Grillenburg	394	GRA	-35.42	0.75	0.87	0.37	0.3
Rollesbroich	457		-26.79	0.81	0.9	0.55	0.49
Schechenfilz Nord	737		2.61	0.68	0.83	0.67	0.82
Spreewald	269	WET	-50.54	0.82	0.91	0.18	0.16
Zarnekow	38		21.62	0.84	0.92	0.77	0.7
Anklam	23		-40.91	0.63	0.79	0.28	0.2

260

261 **3.2. Understanding the water-carbon coupling across Germany**

262 **3.2.1. Spatial variation of ET from 2001 - 2019**

263 Over a nineteen-year period, the mean annual ET across Germany ranges between 250 to 800 mm yr<sup>-1</sup> and has a spatial  
264 mean and standard deviation of 530 ± 49.5 mm yr<sup>-1</sup>. Eastern Germany (Saxony Anhalt, Brandenburg, Mecklenburg  
265 Vorpommern, Saxony, and Thuringia) have lower ET than the spatial mean, while the South and West has higher ET,  
266 as shown in Fig. 4a. On an annual scale, Bavaria and Lower Saxony experiences significant ET losses. The absolute  
267 losses are 39.5 billion m<sup>3</sup> yr<sup>-1</sup> in Bavaria and 25.7 billion m<sup>3</sup> yr<sup>-1</sup> in Lower Saxony. Bavaria has a smaller fraction of  
268 its precipitation lost as ET (0.3 to 0.9) compared to Lower Saxony (0.5 to 0.9). Across Germany, the eastern states  
269 lost the largest share of their precipitation as ET (0.8 – 1.0), leading to a very limited available water supply in the  
270 region, shown in Fig. 4b. Furthermore, to understand whether ET is limited by energy or water availability, we  
271 estimated ET:PET ratio across Germany. PET is the atmospheric evaporative demand under ideal conditions (i.e., no  
272 soil water stress) and acts as an upper limit of ET. The actual ET of watersheds near the Alps exceeds the PET due to  
273 high precipitation, saturated soils and land cover type. These watersheds receive more precipitation compared to the  
274 rest therefore energy limits the ET values, while for the rest parts of Germany the water availability limits ET (Fig.  
275 4c). Lastly, eastern states and some watersheds in Rhineland-Pfalz and Hessen are drier with relatively high-water  
276 scarcity as they receive less precipitation compared to their PET (Fig. 4d).

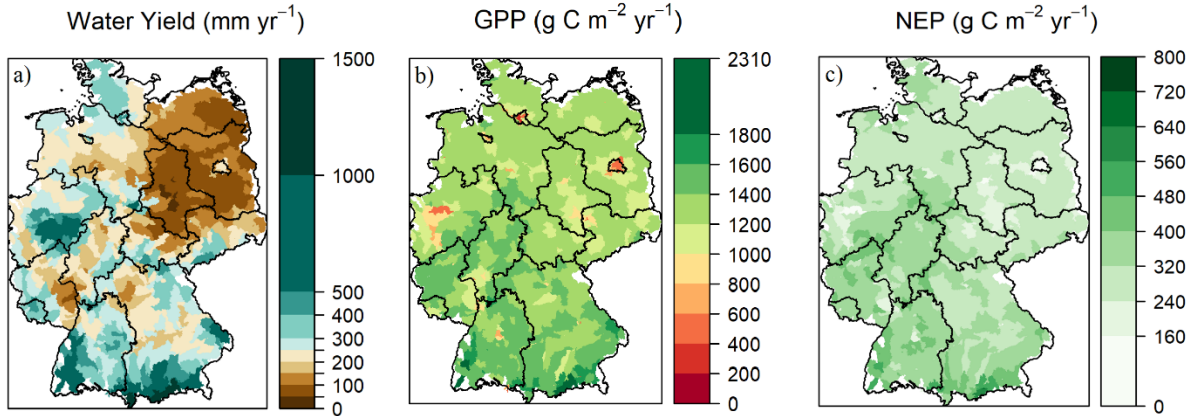


277

278 **Figure 4:** Modelled parameters presenting ET dynamics on a watershed scale across Germany over state boundaries  
 279 within the period of 2001 - 2019. The separate sections show a) mean annual actual ET (mm yr<sup>-1</sup>), b) ratios between  
 280 ET and precipitation, c) ratios between ET and potential ET and d) ratios between precipitation and potential ET.

### 281 3.2.2. Ecosystem services across Germany throughout 2001 – 2019.

282 The mean annual water yield across Germany ranges between 31.8 – 1477.5 mm yr<sup>-1</sup>, has a spatial average of 259 ±  
 283 173.5 mm yr<sup>-1</sup> and generates a total discharge of 84.86 billion m<sup>3</sup> per year (Fig. 5a). In eastern states the water yield  
 284 is lower than the spatial average, while in southern states it is higher. The mean annual GPP estimates (Fig. 5b) are  
 285 found between 0 – 2046.5 g C m<sup>-2</sup> yr<sup>-1</sup> with a spatial average of 1278.8 ± 237.7 g C m<sup>-2</sup> yr<sup>-1</sup> and a total national carbon  
 286 uptake of 441.54 Tg C yr<sup>-1</sup>. The mean annual NEP values (Fig. 5c) are observed between 0 – 665.5 g C m<sup>-2</sup> yr<sup>-1</sup> with  
 287 a spatial average of 308.3 ± 78.2 g C m<sup>-2</sup> yr<sup>-1</sup> and a total national carbon sequestration of 106.03 Tg C yr<sup>-1</sup>.

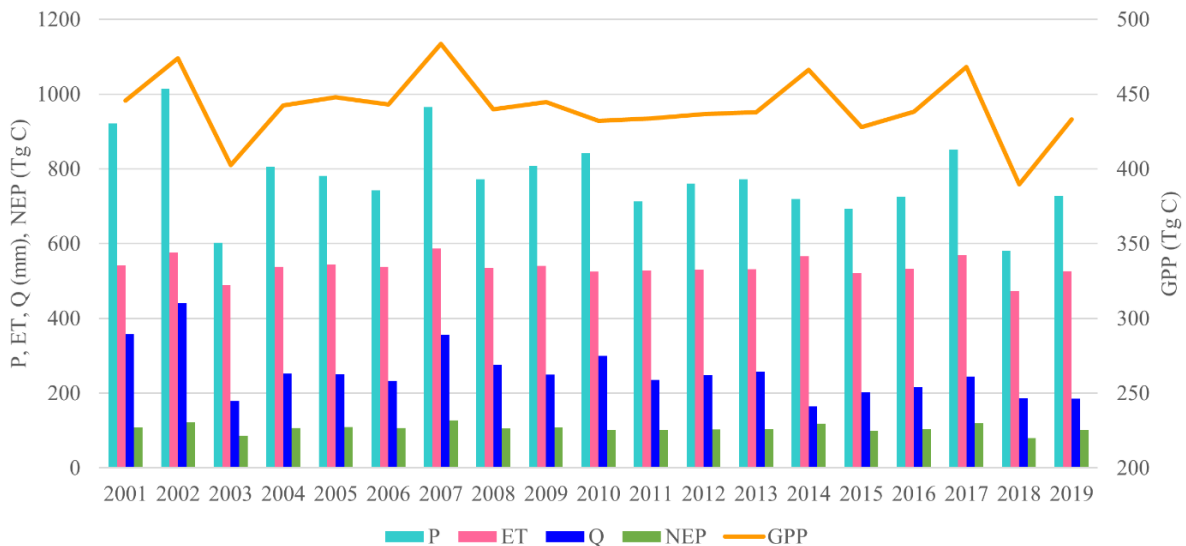


288

289 **Figure 5:** Spatial distribution of model simulated **a)** mean annual total water yield (mm yr<sup>-1</sup>), **b)** mean annual GPP (g C  
290 m<sup>-2</sup> yr<sup>-1</sup>), and **c)** mean annual NEP (g C m<sup>-2</sup> yr<sup>-1</sup>).

291 **3.2.3. Temporal variability of ecosystem services and the control of land cover on these services.**

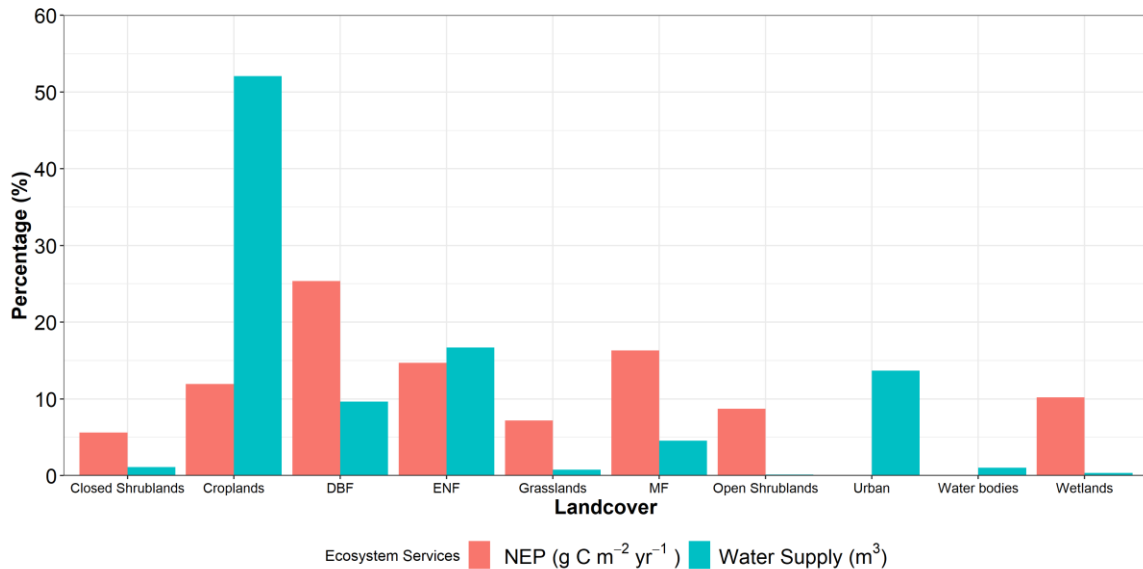
292 The mean annual precipitation for the period 2001–2019 is estimated at 779 ± 106.2 mm/year. Notably, 2002 and  
293 2007 are identified as the two wettest years within this timeframe. Precipitation in 2002 exceeded the mean by 30.2%,  
294 while in 2007 it was 24% higher than the mean. Conversely, the driest years are 2003 and 2018, with rainfall falling  
295 below the mean by 22.7% and 25.5%, respectively. There are relatively high variations in Q and NEP during these  
296 wet and dry years, indicating that these two fluxes are sensitive to changes in precipitation compared to ET and GPP.  
297 In 2018, which is the driest year in the study period, we observed that compared to the mean there is 25.5% less  
298 precipitation. This is accompanied by 11.7% less ET, a 26.8% reduction in Q, 11.7% less GPP and 24.7% lower NEP.  
299 Alternatively, during 2002, the wettest year in our study, we found 30.2% more precipitation compared to mean.  
300 Which may have lead to 7.4% more in ET, 73.4% higher Q, 7.3% more GPP, and 15.5% rise in NEP, relative to mean.  
301 An annual overview for temporal variation is presented in Fig. 6.



302

303 **Figure 6:** Simulated annual ecosystem fluxes evapotranspiration ET (mm), Net ecosystem productivity NEP (Tg C)  
304 ), Gross Primary Productivity GPP (Tg C), discharge Q (mm) and precipitation P (mm) across Germany simulated  
305 by the model during 2001 - 2019.

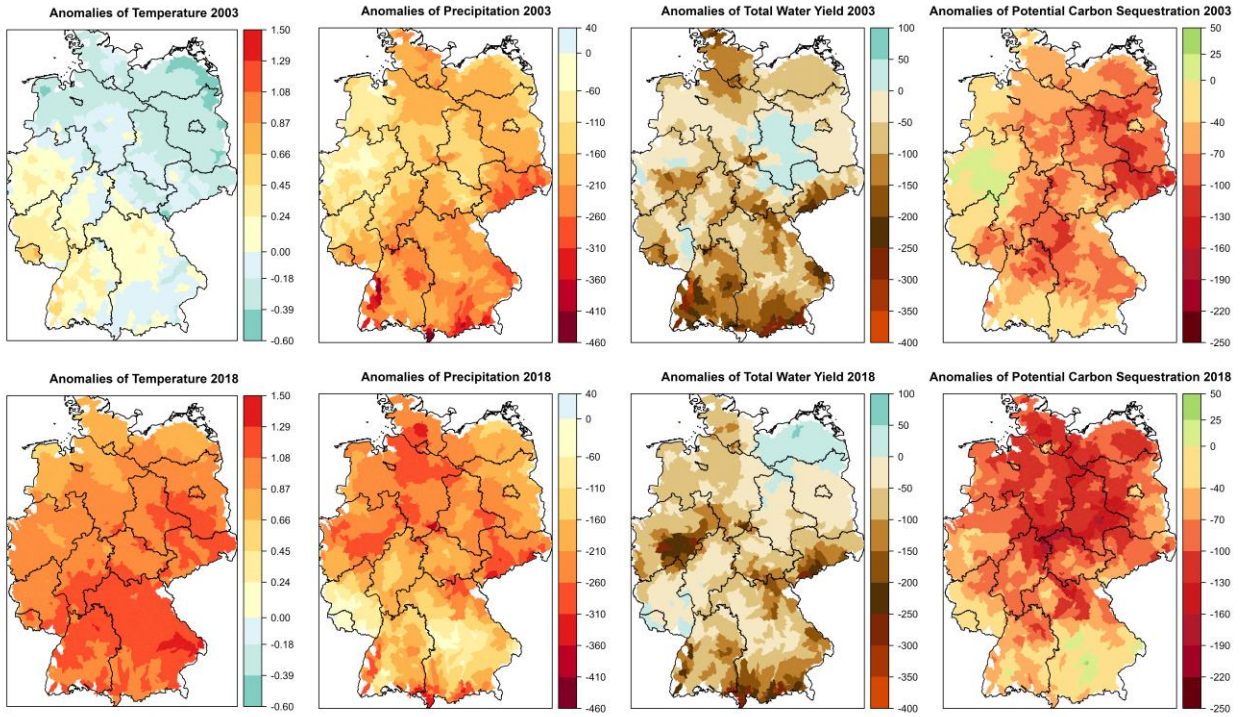
306 To evaluate the role of land cover in water yield and carbon sequestration, we estimated the share of ecosystem services  
 307 provided by the ten different land cover classes. The most essential land covers that provide the largest share of water  
 308 across Germany are Cropland (52.1%), ENF (16.7%), and Urban (13.7%); they supply 82.5% of the water in total.  
 309 Furthermore, forest sequester most of the carbon DBF (25.3%), mixed forest (MF) (16.3%), and ENF (14.7%). They  
 310 contribute 56.3% of carbon sequestered in Germany while only accounting for 30.5% of the land cover. Lastly, we  
 311 would like to highlight that a small portion of land covers, such as wetlands, open shrubland, closed shrubland, and  
 312 grasslands cover less than 2% of German territory; however, they regulate > 30% of the total carbon sequestered in  
 313 Germany, indicating the high importance of conserving these ecosystems, as shown in Fig. 7.



314 **Figure 7:** Simulated mean percentage or share of carbon sequestration and water supply originating from different  
 315 land covers across Germany.  
 316

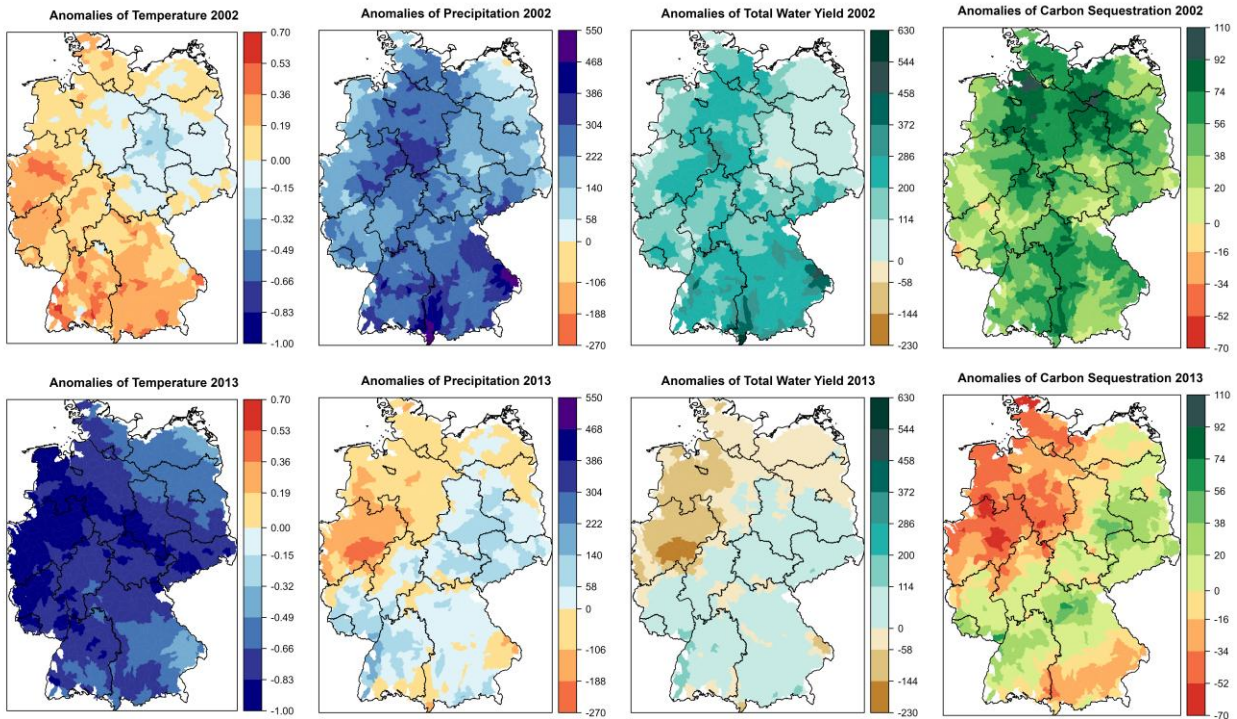
### 317 3.2.4. Spatial variability of ecosystem services during extreme weather events

318 To understand the impact of droughts and extreme precipitation on ecosystem services, we examined the droughts for  
 319 the year 2003 & 2018 and the extremely wet years 2002 and 2013. During 2003, precipitation was 22.7% less than its  
 320 average and only western states had close to average precipitation. The total water yield was 29.6% less than average.  
 321 The carbon sequestration was 18.5% lower than average. While western states had close to average carbon  
 322 sequestration the rest experienced significantly reduced levels. Compared to 2003, the pattern and intensity of the  
 323 2018 drought was more severe. During this event, Germany cumulatively received 25.5% less precipitation, had a  
 324 26.8% lower water yield, and had 24.7% less carbon sequestration. The total water yield was 62.13 billion m<sup>3</sup>, total  
 325 carbon uptake was 389.77 TgC, and total carbon sequestration was 79.82 TgC. The variations in ecosystem services  
 326 due to both drought events are presented in Fig. 8. On the other hand, during the extremely wet year of 2002, Germany  
 327 received 30% more precipitation than annual mean. The water yield and carbon sequestration were 70% and 15.5%  
 328 higher than the mean, respectively. The second wet year of 2013 suffered from severe regional floods. The regions  
 329 that received higher precipitation had a larger water yield and sequestered more carbon. Interestingly, northwest  
 330 Germany was drier than the mean, as a result, the overall ecosystem services for 2013 were close to the mean estimates.  
 331 The variations in ecosystem services during both years are presented in Fig. 9. Similar patterns were observed in the  
 332 standardized anomaly plots presented in Fig. S4 and Fig. S5.



333  
 334  
 335  
 336  
 337  
 338

**Figure 8:** The response of ecosystem services, water yield (mm) and carbon sequestration (g C m<sup>-2</sup>), during two drought events (2003 and 2018). Both drought events had different spatial patterns and intensities, thus the response from the ecosystem varied spatially. The anomalies in the figure were estimated by subtracting the mean annual values for the period 2001 – 2019 from the estimates of the individual drought years 2003 and 2018 on a watershed scale. The temperature anomalies (°C) are also provided for understanding the events.



339  
 340 **Figure 9:** The response of ecosystem services, water yield (mm) and carbon sequestration ( $\text{g C m}^{-2}$ ), during two  
 341 extreme precipitation events (2002 and 2013). Both events had different spatial patterns and intensities, thus the  
 342 response from the ecosystem varied spatially. The anomalies in the figure were estimated by subtracting the mean  
 343 annual values for the period 2001 – 2019 from the estimates of the individual years 2002 and 2013 on a watershed  
 344 scale. The temperature anomalies ( $^{\circ}\text{C}$ ) are also provided for understanding the events.

#### 345 4. Discussion

346 This study explores the response of water-carbon cycle to land cover and extreme events across Germany on watershed  
 347 scale. The WaSSI model performs reasonably well in this region and is estimated to generate 84.86 billion  $\text{m}^3$  of  
 348 discharge and 106.03 TgC of carbon sequestration per year. The results (Figure 7) also highlight the importance of  
 349 sparse landcovers (e.g. wetlands, open shrubland, closed shrubland, and grasslands) in regulating carbon sequestration.  
 350 Furthermore, the study shows that ecosystem services are quite sensitive to droughts and extreme precipitation events,  
 351 but buffers developed from the previous year can play a significant role in mitigating this effect. As shown in Figure  
 352 8, we observe low but positive water yield anomalies during drought years in parts of Germany. Buffers can help delay  
 353 the onset of hydrological droughts in the region.

354 The model validation results successfully demonstrate that the model can be applied across Germany. Furthermore,  
 355 due to the common climatic and hydrological regime, we believe the model can potentially be applied to a broader  
 356 central European region. The simulated discharge had small model bias percentage and high regression values.  
 357 Furthermore, the spatial and temporal variability of the discharge was modelled reasonably well with high NSE, KGE,  
 358  $R^2$  and low P-bias for most watersheds (Table S3 - S4). Except for station Wasserthaleben, which had very high flow  
 359 values leading to a P-bias equal to 131.8%, KGE of -1.48, and annual  $R^2$  of 0.18. The poor performance of this  
 360 individual station could be attributed to several possible reasons, including its relatively small surface area, the  
 361 uncertainty of input data (soil parameters or climate data), underestimation of losses to groundwater, simplification of  
 362 physical processes that estimate surface runoff, or the presence of prevalent unidentified dams in the watershed  
 363 (Caldwell et al., 2012).

364 Simulated ET validated reasonably well against data from different eddy flux towers across the study area (Fig. 3).  
 365 The largest discrepancy was found in Lackenberg station. Even though corrected ET values are used for validation,  
 366 there might be uncertainties in correction factor (Pastorello et al., 2020) and inaccuracies in the observed data due to

367 energy imbalance. For spatial analysis, the simulated ET was compared with MODIS data. The model values were  
368 low compared to MODIS ET in southern and northwestern Germany, but high in mid-western and eastern Germany.  
369 The discrepancies between MODIS-ET and WaSSI ET could be attributed to multiple factors, i.e. the intrinsic  
370 limitations of the different algorithms used by the model and MODIS to estimate ET, uncertainty from the  
371 misclassification of land cover between the two datasets, uncertainties in the model's input data, uncertainties in  
372 MODIS's input data, exclusion of waterbodies in ET estimation by MODIS, and the role of interception in MODIS-  
373 ET estimation (Kim et al., 2012; Trambauer et al., 2014).

374 Furthermore, the model performance across different land covers showed that simulated GPP estimates capture forest  
375 biomes significantly well, except for the station in Lackenberg Forest. The model performance for the rest of the land  
376 covers was less straightforward. For example, croplands had good model biases but low regression values; grasslands  
377 had poor model biases, but high regression estimates; wetlands are more multifaceted (see Table 1). The discrepancies  
378 in the results can be from 1) the model's inherent limitation i.e., lack of radiation in model PET leading to  
379 underestimation of GPP, 2) an insufficient number of eddy flux data for different land covers, and uncertainty in eddy  
380 flux GPP. The uncertainty of daily GPP can reach 15% to 20% (Falge et al., 2002; Hagen et al., 2006; Lasslop et al.,  
381 2010; Verma et al., 2014). Understanding uncertainties in eddy flux GPP is ongoing research. The mismatch of land  
382 cover and landscape heterogeneity at the evaluation sites between the model (watershed scale) and the eddy flux  
383 (single location) will reduce as more data becomes available with time (Verma et al., 2014). Lastly, the difference  
384 between spatial distribution of simulated GPP and remotely sensed GPP may be due to WUE parameters. They were  
385 derived from the global FLUXNET database, which might not have sufficient representation of certain ecosystems  
386 (e.g., wetlands and savannas) resulting in a bias of GPP estimation (Sun et al., 2011). Nevertheless, multiple studies  
387 have also shown that data from remote sensing tends to underestimate GPP (Liu et al., 2015; Wang et al., 2017; Zhu  
388 et al., 2018).

389 The simulated stocks and flows of ecosystem services across Germany by this study were similar to Zink et al. (2016)  
390 and Huang et al. (2010) who reported annual ET and water scarcity patterns at individual sites. The eastern region  
391 in Germany generally receives less precipitation, has high mean annual temperature, high ET from forests and low  
392 water yield, implying intense water use competition. The total water supply reported by German Environment Agency  
393 (UBA) was higher than the simulated results because WaSSI model does not consider transboundary flows (J. Arle et  
394 al., 2018). Furthermore, the southern region in Germany had slightly higher carbon uptake and sequestration values  
395 than the rest of the country. The distribution patterns of carbon sequestration were similar to carbon uptake because  
396 NEP and GPP have a linear relationship. Urban areas sequestered limited carbon but played a significant role in  
397 altering water balances. The distribution and management of land use and land cover determine how ecosystem  
398 services vary. To ensure adequate quantity and quality of services, like freshwater and natural sink of CO<sub>2</sub>, land use  
399 decision-making must incorporate the assessment of currently available stocks and their actual value according to  
400 regional and national priorities. Based on historical data, the available stocks quantified in this study provide evidence  
401 to relevant stakeholders of different regions. Furthermore, the significance of minor land covers or ecosystems in  
402 terms of proportional coverage, such as wetlands, is also highlighted. Germany aims to become CO<sub>2</sub> neutral by 2045;  
403 synergies and tradeoffs of ecosystem services can be used to design land use policy that align with Sustainable  
404 Development Goals. A science-based approach will be necessary to leverage the potential of natural C sink to fix and  
405 offset carbon emissions.

406 As the frequency and intensity of periodic dry and wet spells change due to global warming so does their impact  
407 through drought and extreme precipitation events. In this work, we, quantified the response of water yield and carbon  
408 sequestration to extreme drought and high precipitation events across Germany. During the drought events of 2003  
409 and 2018, the lack of precipitation, overall, had a direct negative impact on water yield and carbon sequestration. But  
410 it is interesting to see that soil has stored water from the previous years, acting as a buffer and provide limited relief  
411 during extreme drought events (Fig. 8). According to Ciais et al. (2005), a 30% reduction in carbon uptake was  
412 observed across Europe during the drought of 2003, while we estimated a reduction of around 8.8% for Germany.  
413 Europe-wide studies on the impacts of the 2018 drought event on carbon sequestration are presented by Thompson et  
414 al. (2020) and Smith et al. (2020). They found that the annual sequestration anomaly in 2018 across northern Europe  
415 was  $0.02 \pm 0.02$  PgC yr<sup>-1</sup> less compared to a 10-year European mean (Thompson et al., 2020). It was estimated that  
416 during the year 2018 an overall reduction in sequestration was around 57 TgC (Smith et al., 2020). However, a direct  
417 comparison between our research is difficult due to the difference in the spatial boundaries. In general, Germany has  
418 no shortage of water, however, a trend to have less precipitation during summer seasons or prolonged dry spells during

419 main vegetation growing months can have substantial adverse effects on both surface water and groundwater supply.  
420 Temporary seasonal rainfall deficiency can cause significant losses of surface water supply and carbon sequestration,  
421 leading to dry conditions that negatively affect the yields and products from the agriculture and forestry sectors. For  
422 example, low soil water availability weakens forest health and favors bark beetle infestation, resulting in huge  
423 economic losses of timber values and forest areas in Germany over the last few years (Lausch et al., 2013;  
424 Zimmermann & Hoffmann, 2020) and the situation continues to worsen. Therefore, land use transformation to adapt  
425 to climate change is indispensable to developing ecological resiliency based on an improved understanding of the role  
426 of various land covers in providing ecosystem services.

427 While this study provides valuable insights on response of water-carbon cycle to land cover and extreme events, it is  
428 limited by the scope of WaSSI Model. The monthly temporal resolution of the model prevents it from estimating peak  
429 flows accurately. The use of WUE to connect ET and carbon sequestration is limited due to insufficient eddy flux  
430 tower coverage. The lack of transboundary river flow and omission of crop rotation further limits the application of  
431 this model. In future, we plan to use WaSSI model across hydrological boundaries, apply projected climate data and  
432 projected landcover data to run simulations for different scenarios. The analysis will help us evaluate future changes  
433 in ecosystem services.

## 434 **5. Conclusions**

435 This study presents new insights into the relationship between water-carbon cycle and land cover, and the impacts of  
436 climate extremes across Germany. The model validation results holistically show that the simple water and carbon  
437 model could capture ecosystem services reasonably well at the national level. Furthermore, the spatial and temporal  
438 relationship between carbon and water highlighted that the eastern states of Germany are comparatively drier than the  
439 rest of the country because most of their precipitation is lost as ET. Nationally, ecosystems in Germany generates a  
440 total annual discharge of 84.86 billion m<sup>3</sup> and sequester 106Tg C yr<sup>-1</sup> carbon. Croplands supply the largest percentage  
441 of available water, while forests sequester the major share of carbon. Minor land covers (e.g. wetlands, open  
442 shrubland, closed shrubland, and grasslands) are also very important in providing ecosystem services for carbon  
443 sequestration. The extreme events in 2003 and 2018 had a significant impact on ecosystem services at the national  
444 level. Moreover, the severe flood of 2013 also played a major role on a regional scale in the Elbe and Danube River  
445 basins. This rigorously verified model provides confidence that the model can be used to strategic applications for  
446 developing Nature-based Solutions (NbS), which will be helpful for Germany to meet its net-zero carbon emissions  
447 by 2050.

448 **6. Acknowledgment**

449 This work was supported by the German Academic Exchange Service (DAAD) PPP Grant (Projekt-ID: 57510261).  
450 We appreciate the funding support from UNU-FLORES and the generous support provided by the US partner – the  
451 Southern Research Station of the United States Forest Service. We also would like to thank the Thünen Institute of  
452 Forest Ecosystems for collaboration.

453 **7. Data Availability**

454 Model software (Liu, 2021), output data (Pyarali, 2024b) and corresponding watershed shapefile (Pyarali, 2024a) used  
455 and prepared in this study are available open source via figshare and can be access from the links in reference list.

456 **8. Author Contributions**

457 *Karim Pyarali*: Writing, review & editing manuscript, Methodology, Investigation, Data curation, Conceptualization.  
458 *Lulu Zhang*: Review, Supervision, Methodology, Funding acquisition, Conceptualization. *Ge Sun*: Review,  
459 Supervision, Methodology, Conceptualization. *Ning Liu*: Review, Data curation, Methodology. *Abdulhakeem Al-*  
460 *Qubati*: Review, Data curation, Methodology.

461 **9. Competing Interests:**

462 The authors declare that they have no known competing financial interests or personal relationships that could have  
463 appeared to influence the work reported in this paper.

464 **10. Reference**

- 465 Allan, A., Soltani, A., Abdi, M. H., & Zarei, M. (2022). Driving Forces behind Land Use and Land Cover Change: A  
466 Systematic and Bibliometric Review. *Land*, 11(8), 1222. <https://doi.org/10.3390/land11081222>
- 467 Al-Qubati, A., Zhang, L., & Pyarali, K. (2023). Climatic drought impacts on key ecosystem services of a low mountain  
468 region in Germany. *Environmental Monitoring and Assessment*, 195(7), 800. [https://doi.org/10.1007/s10661-](https://doi.org/10.1007/s10661-023-11397-1)  
469 [023-11397-1](https://doi.org/10.1007/s10661-023-11397-1)
- 470 Anderson, R. M., Koren, V. I., & Reed, S. M. (2006). Using SSURGO data to improve Sacramento Model a priori  
471 parameter estimates. *Journal of Hydrology*, 320(1–2), 103–116.  
472 <https://doi.org/10.1016/J.JHYDROL.2005.07.020>
- 473 Arowolo, A. O., Deng, X., Olatunji, O. A., & Obayelu, A. E. (2018). Assessing changes in the value of ecosystem  
474 services in response to land-use/land-cover dynamics in Nigeria. *Science of The Total Environment*, 636, 597–  
475 609. <https://doi.org/10.1016/j.scitotenv.2018.04.277>
- 476 Averyt, K., Fisher, J., Huber-Lee, A., Lewis, A., Macknick, J., Madden, N., Rogers, J., & Tellinghuisen, S. (2011).  
477 *Freshwater Use by U.S. Power Plants. Electricity's Thirst for a Precious Resource*.
- 478 Beer, C., Reichstein, M., Ciais, P., Farquhar, G. D., & Papale, D. (2007). Mean annual GPP of Europe derived from  
479 its water balance. *Geophysical Research Letters*, 34(5). <https://doi.org/10.1029/2006GL029006>
- 480 Brown de Colstoun, E. C., C. Huang, P. Wang, J. C. Tilton, B. Tan, J. Phillips, S. Niemczura, P.-Y. Ling, & R. E.  
481 Wolfe. (2017). *Global Man-made Impervious Surface (GMIS) Dataset From Landsat, v1: Global High*  
482 *Resolution Urban Data from Landsat*. Palisades, NY: NASA Socioeconomic Data and Applications Center  
483 (SEDAC).
- 484 Büttner, G., Kosztra, B., Maucha, G., Pataki, R., Kleeschulte, S., Hazeu, G., Vittek, M., Schröder, C., & Littkopf, A.  
485 (2021). *Copernicus Land Monitoring Service CORINE Land Cover (User Manual)*.  
486 <https://land.copernicus.eu/pan-european/corine-land-cover/clc2018?tab=mapview>
- 487 Caldwell, P., Muldoon, C., Ford-Miniat, C., Cohen, E., Krieger, S., Sun, G., McNulty, S., & Bolstad, P. V. (2014).  
488 *Quantifying the role of National Forest System lands in providing surface drinking water supply for the Southern*  
489 *United States*. <https://doi.org/10.2737/SRS-GTR-197>
- 490 Caldwell, P., Sun, G., McNulty, S. G., Cohen, E., & Moore Myers, J. a. (2011). Modeling impacts of environmental  
491 change on ecosystem services across the conterminous United States. *The Fourth Interagency Conference on*  
492 *Research in the Watersheds*, Fairbanks, AK, USA.  
493 [http://admin.forestthreats.org/products/publications/Modeling\\_impacts\\_of\\_environmental\\_change.pdf](http://admin.forestthreats.org/products/publications/Modeling_impacts_of_environmental_change.pdf)
- 494 Caldwell, P. V., Sun, G., McNulty, S. G., Cohen, E. C., & Moore Myers, J. A. (2012). Impacts of impervious cover,  
495 water withdrawals, and climate change on river flows in the conterminous US. *Hydrology and Earth System*  
496 *Sciences*, 16(8), 2839–2857. <https://doi.org/10.5194/hess-16-2839-2012>
- 497 Camacho, F., & Cernicharo, J. (2014). Gio Global Land Component - Lot I "Operation of the Global Land  
498 Component". In *Algorithm Theoretical Basis Document, Issue II.01*.  
499 [http://land.copernicus.eu/global/sites/default/files/products/GIOGL1\\_ATBD\\_SAV1\\_II.01.pdf](http://land.copernicus.eu/global/sites/default/files/products/GIOGL1_ATBD_SAV1_II.01.pdf)
- 500 Chen, D., Liu, N., Gan, G., Liu, Y., Qin, M., Zheng, Q., Sun, G., & Hao, L. (2024). Combined effects of urbanization  
501 and climate variability on water and carbon balances in a rice paddy-dominated basin in southern China.  
502 *Environmental Research Letters*, 19(12), 124042. <https://doi.org/10.1088/1748-9326/ad8a73>
- 503 Cheng, L., Zhang, L., Wang, Y. P., Canadell, J. G., Chiew, F. H. S., Beringer, J., Li, L., Miralles, D. G., Piao, S., &  
504 Zhang, Y. (2017). Recent increases in terrestrial carbon uptake at little cost to the water cycle. *Nature*  
505 *Communications* 2017 8:1, 8(1), 1–10. <https://doi.org/10.1038/s41467-017-00114-5>

- 506 Ciais, P., Reichstein, M., Viovy, N., Granier, A., Ogée, J., Allard, V., Aubinet, M., Buchmann, N., Bernhofer, C.,  
507 Carrara, A., Chevallier, F., De Noblet, N., Friend, A. D., Friedlingstein, P., Grünwald, T., Heinesch, B.,  
508 Keronen, P., Knohl, A., Krinner, G., ... Valentini, R. (2005). Europe-wide reduction in primary productivity  
509 caused by the heat and drought in 2003. *Nature* 2005 437:7058, 437(7058), 529–533.  
510 <https://doi.org/10.1038/nature03972>
- 511 Cui, F., Wang, B., Zhang, Q., Tang, H., De Maeyer, P., Hamdi, R., & Dai, L. (2021). Climate change versus land-use  
512 change—What affects the ecosystem services more in the forest-steppe ecotone? *Science of The Total*  
513 *Environment*, 759, 143525. <https://doi.org/10.1016/j.scitotenv.2020.143525>
- 514 Donmez, C., Sahingoz, M., Paul, C., Cilek, A., Hoffmann, C., Berberoglu, S., Webber, H., & Helming, K. (2024).  
515 Climate change causes spatial shifts in the productivity of agricultural long-term field experiments. *European*  
516 *Journal of Agronomy*, 155, 127121. <https://doi.org/10.1016/j.eja.2024.127121>
- 517 DWD. (2018). *Grids of monthly averaged daily air temperature (2m) over Germany*.  
518 [https://opendata.dwd.de/climate\\_environment/CDC/grids\\_germany/monthly/](https://opendata.dwd.de/climate_environment/CDC/grids_germany/monthly/)
- 519 EEA. (2021). *CLC 2018 — Copernicus Land Monitoring Service*. <https://land.copernicus.eu/pan-european/corine-land-cover/clc2018>
- 521 Eisenreich, S. J. (2005). *Climate Change and the European Water Dimension. A report to the European Water*  
522 *Directors 2005. EU Report No. 21553*. <https://cetesb.sp.gov.br/proclima/2005/05/09/climate-change-and-the-european-water-dimension-a-report-to-the-european-water-directors/>  
523
- 524 Falge, E., Baldocchi, D., Tenhunen, J., Aubinet, M., Bakwin, P., Berbigier, P., Bernhofer, C., Burba, G., Clement, R.,  
525 Davis, K. J., Elbers, J. A., Goldstein, A. H., Grelle, A., Granier, A., Gumundsson, J., Hollinger, D., Kowalski,  
526 A. S., Katul, G., Law, B. E., ... Wofsy, S. (2002). Seasonality of ecosystem respiration and gross primary  
527 production as derived from FLUXNET measurements. *Agricultural and Forest Meteorology*, 113(1–4), 53–74.  
528 [https://doi.org/10.1016/S0168-1923\(02\)00102-8](https://doi.org/10.1016/S0168-1923(02)00102-8)
- 529 Fang, Y., Sun, G., Caldwell, P., McNulty, S. G., Noormets, A., Domec, J., King, J., Zhang, Z., Zhang, X., Lin, G.,  
530 Zhou, G., Xiao, J., & Chen, J. (2015). Monthly land cover-specific evapotranspiration models derived from  
531 global eddy flux measurements and remote sensing data. *Ecohydrology*, 9(2), 248–266.  
532 <https://doi.org/10.1002/eco.1629>
- 533 *Fourth Federal Forest Inventory 2022*. (2024). <https://www.bundeswaldinventur.de/vierte-bundeswaldinventur-2022/vorwort>  
534
- 535 Gentine, P., Green, J. K., Guérin, M., Humphrey, V., Seneviratne, S. I., Zhang, Y., & Zhou, S. (2019). Coupling  
536 between the terrestrial carbon and water cycles—a review. *Environmental Research Letters*, 14(8), 083003.  
537 <https://doi.org/10.1088/1748-9326/AB22D6>
- 538 Gutsch, M., Lasch-Born, P., Kollas, C., Suckow, F., & Reyer, C. P. O. (2018). Balancing trade-offs between ecosystem  
539 services in Germany's forests under climate change. *Environmental Research Letters*, 13(4), 045012.  
540 <https://doi.org/10.1088/1748-9326/aab4e5>
- 541 Hagen, S. C., Braswell, B. H., Linder, E., Frohking, S., Richardson, A. D., & Hollinger, D. Y. (2006). Statistical  
542 uncertainty of eddy flux - Based estimates of gross ecosystem carbon exchange at Howland Forest, Maine.  
543 *Journal of Geophysical Research Atmospheres*, 111(8), 1–12. <https://doi.org/10.1029/2005JD006154>
- 544 Hasan, S. S., Zhen, L., Miah, Md. G., Ahamed, T., & Samie, A. (2020). Impact of land use change on ecosystem  
545 services: A review. *Environmental Development*, 34, 100527. <https://doi.org/10.1016/j.envdev.2020.100527>
- 546 Huang, S., Krysanova, V., Österle, H., & Hattermann, F. F. (2010). Simulation of spatiotemporal dynamics of water  
547 fluxes in Germany under climate change. *Hydrological Processes*, 24(23), 3289–3306.  
548 <https://doi.org/10.1002/HYP.7753>

- 549 J. Arle, H. Bartel, C. Baumgarten, A. Bertram, R. Wolter, G. Winkelmann-Oei, & C. Winde. (2018). *Water Resource*  
550 *Management in Germany: Fundamentals, Pressures, Measures.*  
551 <https://www.umweltbundesamt.de/en/publikationen/water-resource-management-in-germany>
- 552 Jin, K., Liu, N., Tang, R., Sun, G., & Hao, L. (2025). Quantifying Long Term (2000–2020) Water Balances Across  
553 Nepal by Integrating Remote Sensing and an Ecohydrological Model. *Remote Sensing*, 17(11), 1819.  
554 <https://doi.org/10.3390/rs17111819>
- 555 Jung, M., Reichstein, M., Schwalm, C. R., Huntingford, C., Sitch, S., Ahlström, A., Arneth, A., Camps-Valls, G.,  
556 Ciais, P., Friedlingstein, P., Gans, F., Ichii, K., Jain, A. K., Kato, E., Papale, D., Poulter, B., Raduly, B.,  
557 Rödenbeck, C., Tramontana, G., ... Zeng, N. (2017). Compensatory water effects link yearly global land CO2  
558 sink changes to temperature. *Nature* 2017 541:7638, 541(7638), 516–520. <https://doi.org/10.1038/nature20780>
- 559 Kaspar, F., Müller-Westermeier, G., Penda, E., Mächel, H., Zimmermann, K., Kaiser-Weiss, A., & Deutschländer, T.  
560 (2013). Monitoring of climate change in Germany – data, products and services of Germany’s National Climate  
561 Data Centre. *Advances in Science and Research*, 10(1), 99–106. <https://doi.org/10.5194/asr-10-99-2013>
- 562 Keil, M. (2017). *CORINE Land Cover products for Germany* (Number January).  
563 [https://www.dlr.de/eoc/Portaldata/60/Resources/dokumente/6\\_anw\\_land/CORINE\\_Land\\_Cover\\_products\\_for](https://www.dlr.de/eoc/Portaldata/60/Resources/dokumente/6_anw_land/CORINE_Land_Cover_products_for_Germany_at_DFD.pdf)  
564 [\\_Germany\\_at\\_DFD.pdf](https://www.dlr.de/eoc/Portaldata/60/Resources/dokumente/6_anw_land/CORINE_Land_Cover_products_for_Germany_at_DFD.pdf)
- 565 Kim, H. W., Hwang, K., Mu, Q., Lee, S. O., & Choi, M. (2012). Validation of MODIS 16 global terrestrial  
566 evapotranspiration products in various climates and land cover types in Asia. *KSCE Journal of Civil*  
567 *Engineering*, 16(2), 229–238. <https://doi.org/10.1007/s12205-012-0006-1>
- 568 Kosanic, A., Kavcic, I., van Kleunen, M., & Harrison, S. (2019). Climate change and climate change velocity analysis  
569 across Germany. *Scientific Reports*, 9(1), 2196. <https://doi.org/10.1038/s41598-019-38720-6>
- 570 Lasslop, G., Reichstein, M., Papale, D., Richardson, A., Arneth, A., Barr, A., Stoy, P., & Wohlfahrt, G. (2010).  
571 Separation of net ecosystem exchange into assimilation and respiration using a light response curve approach:  
572 Critical issues and global evaluation. *Global Change Biology*, 16(1), 187–208. [https://doi.org/10.1111/j.1365-](https://doi.org/10.1111/j.1365-2486.2009.02041.x)  
573 [2486.2009.02041.x](https://doi.org/10.1111/j.1365-2486.2009.02041.x)
- 574 Lausch, A., Heurich, M., & Fahse, L. (2013). Spatio-temporal infestation patterns of *Ips typographus* (L.) in the  
575 Bavarian Forest National Park, Germany. *Ecological Indicators*, 31, 73–81.  
576 <https://doi.org/10.1016/J.ECOLIND.2012.07.026>
- 577 Law, B. E., Falge, E., Gu, L., Baldocchi, D. D., Bakwin, P., Berbigier, P., Davis, K., Dolman, A. J., Falk, M., Fuentes,  
578 J. D., Goldstein, A., Granier, A., Grelle, A., Hollinger, D., Janssens, I. A., Jarvis, P., Jensen, N. O., Katul, G.,  
579 Mahli, Y., ... Wofsy, S. (2002). Environmental controls over carbon dioxide and water vapor exchange of  
580 terrestrial vegetation. *Agricultural and Forest Meteorology*, 113(1–4), 97–120. [https://doi.org/10.1016/S0168-](https://doi.org/10.1016/S0168-1923(02)00104-1)  
581 [1923\(02\)00104-1](https://doi.org/10.1016/S0168-1923(02)00104-1)
- 582 Liu, N. (2017). *Changes in Water and Carbon in Australian Vegetation in Response to Climate Change* [Murdoch  
583 University]. <https://researchrepository.murdoch.edu.au/id/eprint/40206/>
- 584 Liu, N. (2021). *R-based Water Supply Stress Index (rWaSSI) model.*  
585 <https://sites.google.com/view/rwassi/home?authuser=0>
- 586 Liu, N., Dobbs, G. R., Caldwell, P. V., Miniati, C. F., Bolstad, P. V., Nelson, S., & Sun, G. (2020). *Quantifying the*  
587 *role of State and private forest lands in providing surface drinking water supply for the Southern United States.*  
588 <https://doi.org/10.2737/SRS-GTR-248>
- 589 Liu, N., SUN, P.-S., Liu, S.-R., & Sun, G. (2013). Determination of spatial scale of response unit for WASSI-C eco-  
590 hydrological model—a case study on the upper Zagunao River watershed of China. *Chinese Journal of Plant*  
591 *Ecology*. <https://doi.org/10.3724/SP.J.1258.2013.00000>

- 592 Liu, Z., Shao, Q., & Liu, J. (2015). The performances of MODIS-GPP and -ET products in China and their sensitivity  
593 to input data (FPAR/LAI). *Remote Sensing*, 7(1), 135–152. <https://doi.org/10.3390/rs70100135>
- 594 Margulis, S. A., Wood, E. F., & Troch, P. A. (2006). The Terrestrial Water Cycle: Modeling and Data Assimilation  
595 across Catchment Scales. *Journal of Hydrometeorology*, 7(3), 309–311. <https://doi.org/10.1175/JHM999.1>
- 596 McCabe, G. J., & Wolock, D. M. (1999). GENERAL-CIRCULATION-MODEL SIMULATIONS OF FUTURE  
597 SNOWPACK IN THE WESTERN UNITED STATES1. *JAWRA Journal of the American Water Resources  
598 Association*, 35(6), 1473–1484. <https://doi.org/10.1111/J.1752-1688.1999.TB04231.X>
- 599 McNulty, S., Cohen, E., Sun, G., & Caldwell, P. (2016). HYDROLOGIC MODELING FOR WATER RESOURCE  
600 ASSESSMENT IN A DEVELOPING COUNTRY: THE RWANDA CASE STUDY. *USDA FOREST  
601 SERVICE*. <https://www.fs.usda.gov/treearch/pubs/53039>
- 602 Morales, P., Sykes, M. T., Prentice, I. C., Smith, P., Smith, B., Bugmann, H., Zierl, B., Friedlingstein, P., Viovy, N.,  
603 Sabaté, S., Sánchez, A., Pla, E., Gracia, C. A., Sitch, S., Arneeth, A., & Ogee, J. (2005). Comparing and  
604 evaluating process-based ecosystem model predictions of carbon and water fluxes in major European forest  
605 biomes. *Global Change Biology*, 11(12), 2211–2233. <https://doi.org/10.1111/J.1365-2486.2005.01036.X>
- 606 Pandey, B., & Ghosh, A. (2023). Urban ecosystem services and climate change: a dynamic interplay. *Frontiers in  
607 Sustainable Cities*, 5. <https://doi.org/10.3389/frsc.2023.1281430>
- 608 Pastorello, G., Trotta, C., Canfora, E., Chu, H., Christianson, D., Cheah, Y. W., Poindexter, C., Chen, J., Elbashandy,  
609 A., Humphrey, M., Isaac, P., Polidori, D., Ribeca, A., van Ingen, C., Zhang, L., Amiro, B., Ammann, C., Arain,  
610 M. A., Ardö, J., ... Papale, D. (2020). The FLUXNET2015 dataset and the ONEFlux processing pipeline for  
611 eddy covariance data. *Scientific Data*, 7(1), 225. <https://doi.org/10.1038/s41597-020-0534-3>
- 612 Potter, C., & Pass, S. (2024). Changes in the net primary production of ecosystems across Western Europe from 2015  
613 to 2022 in response to historic drought events. *Carbon Balance and Management*, 19(1), 32.  
614 <https://doi.org/10.1186/s13021-024-00279-9>
- 615 Prescher, A.-K., Grünwald, T., & Bernhofer, C. (2010). Land use regulates carbon budgets in eastern Germany: From  
616 NEE to NBP. *Agricultural and Forest Meteorology*, 150(7–8), 1016–1025.  
617 <https://doi.org/10.1016/j.agrformet.2010.03.008>
- 618 Pyarali, K. (2024a). *Germany Watershed Delineation*. Figshare.  
619 <https://doi.org/https://doi.org/10.6084/m9.figshare.25053599.v1>
- 620 Pyarali, K. (2024b). *WaSSI Model Output*. Figshare. <https://doi.org/https://doi.org/10.6084/m9.figshare.25053641.v1>
- 621 Running, S. W., Mu, Q., Zhao, M., & Moreno, A. (2019a). *User's Guide Daily GPP and Annual NPP  
622 (MOD17A2H/A3H) and Year-end Gap-Filled (MOD17A2HGF/A3HGF) Products*.  
623 <https://lpdaac.usgs.gov/products/mod17a2hgf006/>
- 624 Running, S. W., Mu, Q., Zhao, M., & Moreno, A. (2019b). *User's Guide MODIS Global Terrestrial  
625 Evapotranspiration (ET) Product NASA Earth Observing System MODIS Land Algorithm (For Collection 6)*.  
626 <https://doi.org/10.5067/MODIS/MOD16A2GF.006>
- 627 Salerno, F., Gaetano, V., & Gianni, T. (2018). Urbanization and climate change impacts on surface water quality:  
628 Enhancing the resilience by reducing impervious surfaces. *Water Research*, 144, 491–502.  
629 <https://doi.org/10.1016/j.watres.2018.07.058>
- 630 Schröter, D., Zebisch, M., & Grothmann, T. (2005). *Climate Change in Germany-Vulnerability and Adaptation of  
631 Climate-Sensitive Sectors*.  
632 [https://www.researchgate.net/publication/232071870\\_Climate\\_Change\\_in\\_Germany-  
633 Vulnerability\\_and\\_Adaptation\\_of\\_Climate-Sensitive\\_Sectors](https://www.researchgate.net/publication/232071870_Climate_Change_in_Germany-Vulnerability_and_Adaptation_of_Climate-Sensitive_Sectors)

- 634 Schumacher, E. (2022, January 10). *Natural disasters cost \$280 billion in 2021: German insurance firm* | News | DW  
635 | 10.01.2022. [https://www.dw.com/en/natural-disasters-cost-280-billion-in-2021-german-insurance-firm/a-](https://www.dw.com/en/natural-disasters-cost-280-billion-in-2021-german-insurance-firm/a-60378575)  
636 [60378575](https://www.dw.com/en/natural-disasters-cost-280-billion-in-2021-german-insurance-firm/a-60378575)
- 637 Smets, B., Swinnen, E., & Van Hoolst, R. (2019). Product User Manual: Dry Matter Productivity and Gross Dry  
638 Matter Productivity. Version 2. Collection 1km. In *Copernicus Global Land Services*.  
639 <https://land.copernicus.eu/global/products/dmp>
- 640 Smith, N. E., Kooijmans, L. M. J., Koren, G., Van Schaik, E., Van Der Woude, A. M., Wanders, N., Ramonet, M.,  
641 Xueref-Remy, I., Siebicke, L., Manca, G., Brümmer, C., Baker, I. T., Haynes, K. D., Luijkx, I. T., & Peters, W.  
642 (2020). Spring enhancement and summer reduction in carbon uptake during the 2018 drought in northwestern  
643 Europe. *Philosophical Transactions of the Royal Society B*, 375(1810).  
644 <https://doi.org/10.1098/RSTB.2019.0509>
- 645 Sun, G., Caldwell, P., Noormets, A., McNulty, S. G., Cohen, E., Myers, J. M., Domec, J.-C., Treasure, E., Mu, Q.,  
646 Xiao, J., John, R., & Chen, J. (2011). Upscaling key ecosystem functions across the conterminous United States  
647 by a water-centric ecosystem model. *Journal of Geophysical Research: Biogeosciences*, 116(G3).  
648 <https://doi.org/10.1029/2010JG001573>
- 649 Sun, G., Wei, X., Hao, L., Sanchis, M. G., Hou, Y., Yousefpour, R., Tang, R., & Zhang, Z. (2023). Forest hydrology  
650 modeling tools for watershed management: A review. *Forest Ecology and Management*, 530(4), 120755-.  
651 <https://doi.org/10.1016/J.FORECO.2022.120755>
- 652 Sun, S., Sun, G., Caldwell, P., McNulty, S. G., Cohen, E., Xiao, J., & Zhang, Y. (2015). Drought impacts on ecosystem  
653 functions of the U.S. National Forests and Grasslands: Part I evaluation of a water and carbon balance model.  
654 *Forest Ecology and Management*, 353, 260–268. <https://doi.org/10.1016/j.foreco.2015.03.054>
- 655 Thompson, R. L., Broquet, G., Gerbig, C., Koch, T., Lang, M., Monteil, G., Munassar, S., Nickless, A., Scholze, M.,  
656 Ramonet, M., Karstens, U., Van Schaik, E., Wu, Z., & Rödenbeck, C. (2020). Changes in net ecosystem  
657 exchange over Europe during the 2018 drought based on atmospheric observations. *Philosophical Transactions*  
658 *of the Royal Society B*, 375(1810). <https://doi.org/10.1098/RSTB.2019.0512>
- 659 Trambauer, P., Dutra, E., Maskey, S., Werner, M., Pappenberger, F., Van Beek, L. P. H., & Uhlenbrook, S. (2014).  
660 Comparison of different evaporation estimates over the African continent. *Hydrology and Earth System*  
661 *Sciences*, 18(1), 193–212. <https://doi.org/10.5194/hess-18-193-2014>
- 662 Turner, D. P., Ritts, W. D., Cohen, W. B., Gower, S. T., Running, S. W., Zhao, M., Costa, M. H., Kirschbaum, A. A.,  
663 Ham, J. M., Saleska, S. R., & Ahl, D. E. (2006). Evaluation of MODIS NPP and GPP products across multiple  
664 biomes. *Remote Sensing of Environment*, 102(3–4), 282–292. <https://doi.org/10.1016/j.rse.2006.02.017>
- 665 Ungaro, F., Schwartz, C., & Piorr, A. (2021). Ecosystem services indicators dataset for the utilized agricultural area  
666 of the Märkisch-Oderland District-Brandenburg, Germany. *Data in Brief*, 34, 106645.  
667 <https://doi.org/10.1016/j.dib.2020.106645>
- 668 Velpuri, N. M., Senay, G. B., Singh, R. K., Bohms, S., & Verdin, J. P. (2013). A comprehensive evaluation of two  
669 MODIS evapotranspiration products over the conterminous United States: Using point and gridded FLUXNET  
670 and water balance ET. *Remote Sensing of Environment*, 139, 35–49. <https://doi.org/10.1016/j.rse.2013.07.013>
- 671 Verger, A., Descals, A., Benhadj, I., & Claes, P. (2018). *Product User Guide and Specification: CDR VGT-based LAI*  
672 *and fAPAR v1.0*. [http://datastore.copernicus-climate.eu/c3s/published-forms/c3sprod/satellite-soil-](http://datastore.copernicus-climate.eu/c3s/published-forms/c3sprod/satellite-soil-moisture/product-user-guide-v2.3.pdf)  
673 [moisture/product-user-guide-v2.3.pdf](http://datastore.copernicus-climate.eu/c3s/published-forms/c3sprod/satellite-soil-moisture/product-user-guide-v2.3.pdf)
- 674 Verma, M., Friedl, M. A., Richardson, A. D., Kiely, G., Cescatti, A., Law, B. E., Wohlfahrt, G., Gielen, B., Rouspard,  
675 O., Moors, E. J., Toscano, P., Vaccari, F. P., Gianelle, D., Bohrer, G., Varlagin, A., Buchmann, N., Van Gorsel,  
676 E., Montagnani, L., & Propastin, P. (2014). Remote sensing of annual terrestrial gross primary productivity from

677 MODIS: An assessment using the FLUXNET la Thuile data set. *Biogeosciences*, 11(8), 2185–2200.  
678 <https://doi.org/10.5194/bg-11-2185-2014>

679 Wang, L., Zhu, H., Lin, A., Zou, L., Qin, W., & Du, Q. (2017). Evaluation of the latest MODIS GPP products across  
680 multiple biomes using global eddy covariance flux data. *Remote Sensing*, 9(5).  
681 <https://doi.org/10.3390/rs9050418>

682 Williams, I. N., Torn, M. S., Riley, W. J., & Wehner, M. F. (2014). Impacts of climate extremes on gross primary  
683 production under global warming. *Environmental Research Letters*, 9(9), 094011. <https://doi.org/10.1088/1748-9326/9/9/094011>

685 Wu, S., Tetzlaff, D., Goldhammer, T., & Soulsby, C. (2021). Hydroclimatic variability and riparian wetland  
686 restoration control the hydrology and nutrient fluxes in a lowland agricultural catchment. *Journal of Hydrology*,  
687 603, 126904. <https://doi.org/10.1016/j.jhydrol.2021.126904>

688 Zeng, Z., Piao, S., Li, L. Z. X., Wang, T., Ciais, P., Lian, X., Yang, Y., Mao, J., Shi, X., & Myneni, R. B. (2018).  
689 Impact of Earth Greening on the Terrestrial Water Cycle. *Journal of Climate*, 31(7), 2633–2650.  
690 <https://doi.org/10.1175/JCLI-D-17-0236.1>

691 Zhang, J., Zhang, Y., Sun, G., Song, C., Li, J., Hao, L., & Liu, N. (2022). Climate Variability Masked Greening Effects  
692 on Water Yield in the Yangtze River Basin During 2001–2018. *Water Resources Research*, 58(1),  
693 e2021WR030382. <https://doi.org/10.1029/2021WR030382>

694 Zhang, L., Cheng, L., Chiew, F., & Fu, B. (2018). Understanding the impacts of climate and landuse change on water  
695 yield. *Current Opinion in Environmental Sustainability*, 33, 167–174.  
696 <https://doi.org/10.1016/J.COSUST.2018.04.017>

697 Zhang, Y., Song, C., Sun, G., Band, L. E., McNulty, S., Noormets, A., Zhang, Q., & Zhang, Z. (2016). Development  
698 of a coupled carbon and water model for estimating global gross primary productivity and evapotranspiration  
699 based on eddy flux and remote sensing data. *Agricultural and Forest Meteorology*, 223, 116–131.  
700 <https://doi.org/10.1016/J.AGRFORMET.2016.04.003>

701 Zhang, Y., Zhang, Z., Reed, S., & Koren, V. (2011). An enhanced and automated approach for deriving a priori SAC-  
702 SMA parameters from the soil survey geographic database. *Computers & Geosciences*, 37(2), 219–231.  
703 <https://doi.org/10.1016/J.CAGEO.2010.05.016>

704 Zhu, X., Pei, Y., Zheng, Z., Dong, J., Zhang, Y., Wang, J., Chen, L., Doughty, R. B., Zhang, G., & Xiao, X. (2018).  
705 Underestimates of grassland gross primary production in MODIS standard products. *Remote Sensing*, 10(11).  
706 <https://doi.org/10.3390/rs10111771>

707 Zimmermann, S., & Hoffmann, K. (2020). Evaluating the capabilities of Sentinel-2 data for large-area detection of  
708 bark beetle infestation in the Central German Uplands. <https://doi.org/10.1117/1.JRS.14.024515>, 14(2),  
709 024515. <https://doi.org/10.1117/1.JRS.14.024515>

710 Zink, M., Kumar, R., Cuntz, M., & Samaniego, L. (2016). A High-Resolution Dataset of Water Fluxes and States for  
711 Germany Accounting for Parametric Uncertainty. *Hydrology and Earth System Sciences Discussions*,  
712 (September), 1–29. <https://doi.org/10.5194/hess-2016-443>

713

714

715

716